Comprehensive Analysis of Chemical Bonding in Boron Clusters

DMITRY YU. ZUBAREV, ALEXANDER I. BOLDYREV
Department of Chemistry and Biochemistry, Utah State University, 0300 Old Main Hill, Logan, UT 84322-0300

Received 27 March 2006; Revised 14 May 2006; Accepted 20 June 2006
DOI 10.1002/jcc.20518
Published online 16 November 2006 in Wiley InterScience (www.interscience.wiley.com).

Abstract: We present a comprehensive analysis of chemical bonding in pure boron clusters. It is now established in joint experimental and theoretical studies that pure boron clusters are planar or quasi-planar at least up to twenty atoms. Their planarity or quasi-planarity was usually discussed in terms of π-delocalization or π-aromaticity. In the current article, we demonstrated that one cannot ignore σ-electrons and that the presence of two-center two-electron (2c—2e) peripheral B—B bonds together with the globally delocalized σ-electrons must be taken into consideration when the shape of pure boron cluster is discussed. The global aromaticity (or global antiaromaticity) can be assigned on the basis of the $4n + 2$ (or $4n$) electron counting rule for either π- or σ-electrons in the planar structures. We showed that pure boron clusters could have double (σ- and π-) aromaticity (B_3^-, B_4, B_5^+, B_6^{2+}, B_7^+, B_7^-, B_8, B_8^{2-}, B_9^-, B_{10}, B_{11}^+, B_{12}, and B_{13}^+), double (σ- and π-) antiaromaticity (B_6^{2-}, B_{15}), or conflicting aromaticity (B_5^-,σ-antiaromatic and π-aromatic and B_{14}, σ-aromatic and π-antiaromatic). Appropriate geometric fit is also an essential factor, which determines the shape of the most stable structures. In all the boron clusters considered here, the peripheral atoms form planar cycles. Peripheral 2c—2e B—B bonds are built up from s to p hybrid atomic orbitals and this enforces the planarity of the cycle. If the given number of central atoms (1, 2, 3, or 4) can perfectly fit the central cavity then the overall structure is planar. Otherwise, central atoms come out of the plane of the cycle and the overall structure is quasi-planar.

 J Comput Chem 28: 251–268, 2007

Key words: boron clusters; aromaticity; double aromaticity; double antiaromaticity; conflicting aromaticity; chemical bonding

Introduction

Homoatomic and heteroatomic clusters today represent the final frontier for developing unified chemical bonding theory.

In organic chemistry, a vast majority of molecules can be represented by a single Lewis structure (classical molecules) with either single or multiple two-center two-electron (2c—2e) bonds and with an appropriate number of lone pairs on electron-rich atoms. Chemical bonding in many inorganic molecules also can be represented by a single Lewis structure, but generally in inorganic chemistry such a description encounters significant problems. If, however, a single Lewis structure description is not sufficient, then the resonance of Lewis structures is used. The last approach is particularly important for description of the chemical bonding in aromatic compounds. The major advantage of the above-mentioned chemical bonding model is that we can predict possible isomers of classical molecules using just paper and pencil and with high certainty we can also predict which isomer could be the most stable one for a given stoichiometry. We can also draw a possible mechanism of chemical reaction using the above-mentioned chemical bonding models, which makes them irreplaceable in chemistry.

However, we do not have similar chemical bonding models allowing us to use the "paper and pencil" approach for predicting isomers of homoatomic and heteroatomic clusters. The brute-force techniques based on genetic algorithm, molecular dynamics, hopping models can help us to find global minima of small clusters as well as their low-lying isomers, but they quickly run into computational problems in larger systems. Without robust chemical bonding models capable of predicting global minimum structures and stable isomers of clusters, our progress in understanding cluster structure and in rational design of molecular/cluster-level electronic and mechanical devices is seriously limited.

Correspondence to: A. I. Boldyrev; e-mail: boldyrev@cc.usu.edu

Contract/grant sponsor: The Petroleum Research Fund, American Chemical Society; contract/grant number: ACS-PRF No. 38242-AC6

Contract/grant sponsor: National Science Foundation; contract/grant numbers: CHE-0404937, CTS-0321170

There was some progress in recent years in developing chemical bonding models for clusters (1–13 and references therein).

Boron clusters are the best understood clusters of the main group elements. Today we are capable of explaining and predicting their geometric structures and other molecular and spectroscopic properties, because of recent advances in developing chemical bonding model for these systems.[5a,6,7b,14–24]

Pioneering works on pure boron cations have been done by Anderson and coworkers.[25–31] These authors produced boron cluster cations in molecular beams using laser vaporization and studied their chemical reactivity and fragmentation properties. They initially postulated the three-dimensional structures for boron clusters. Consequent quantum chemical calculations[32–62] have shown that boron clusters prefer planar or quasi-planar structures. However, these computational predictions were not verified experimentally. In a series of recent articles, joint experimental and theoretical studies have been reported for a number of boron clusters, B_3^- and B_4^-,[14] B_5^-,[15] B_6^-,[16] B_7^-,[17] B_8^- and B_9^-,[18] $B_{10}^- - B_{15}^-$,[19] and their neutrals. The structures of these clusters have been studied computationally and verified through comparisons of experimental and theoretical photoelectron spectra. These studies have confirmed the two-dimensional or quasi two-dimensional structures of all these clusters. Pure boron clusters have been recently reviewed.[63]

Planarity of boron clusters have been primarily discussed in terms of π-delocalization[43,44] and π-aromaticity.[5a,6,7b,14–24] It has been shown, that high symmetric planar boron clusters B_3^- (D_{3h}), B_4 (effectively D_{4h}), B_8^{2-} (D_{7h}), B_9^- (D_{8h}) have either 2 (B_3^- and B_4) or 6 (B_8^{2-} and B_9^-) π-electrons similar to prototypical hydrocarbons $C_3H_3^+$ (D_{3h}, with 2 π-electrons) or C_6H_6 (D_{6h}, with 6 π-electrons), Thus, they formally satisfy the $4n + 2$ Huckel rule and could be considered as π-aromatic clusters. Boron clusters with $4n$ π-electrons such as B_6^{2-} (4 π-electrons) and B_{14} (8 π-electrons) can be considered as π-antiaromatic. Aihara and coworkers[20] recently performed analysis of aromaticity of boron clusters B_x ($x = 3$–15) in terms of topological resonance energy (TRE) and concluded that all boron clusters are highly π-aromatic including systems with $4n$ π-electrons.

To resolve the controversy about aromaticity or antiaromaticity of closed shell boron clusters with $4n$ electrons and also to include σ-electrons into discussion in the current work, we present a comprehensive chemical bonding analysis in the pure boron clusters $B_x^{0,+1,+2,-1,-2}$ ($x = 2$–15). We will consider here only clusters with even number of electrons. For neutral and anionic boron clusters with 3–9 atoms, the σ-aromaticity has been previously considered[14–18,21–24]; however, the influence of σ-electrons on geometric structure of boron clusters with 10–15 atoms have not been discussed yet.[5a,6,19,20] Also, the use of the concept of aromaticity in cationic boron clusters was limited primarily by B_{13}^+ cluster.[5a,6]

Theoretical Methods

In our current study, we used previously determined geometries for B_3^+, B_3^-, B_4, B_4^{2-}, B_5^+, B_5^-, B_6^{2+}, B_6, B_6^{2-}, B_7^+, B_7^-, B_8, B_8^{2-}, B_9^-, B_{10}, B_{11}^+, B_{11}^-, B_{12}, B_{13}^+, B_{14}, and B_{15}^- clusters, which have been summarized in recent review.[63] Their structures are shown in Figure 1. Chemical bonding analysis was preformed using the natural bond analysis (NBO)[64] (at the B3LYP/6-311+G* level of theory[65–69]), pictures of Hatree-Fock canonical MOs (RHF/6-311+G*), and nuclear independent chemical shift (NICS)[70] (B3LYP/6-311 + G*). We also calculated first singlet vertical excitation energies at TD-B3LYP/6-311 + G*[71,72] as a probe of aromaticity or antiaromaticity. All calculations have been performed using Gaussian 03 program.[73] MO pictures were made using the Molden 3.4 program.[74] Results of our calculations are summarized in Table1.

Chemical Bonding Analysis

In our chemical bonding analysis, we adopt the following approach. First, we use the NBO analysis to determine which canonical MOs can be localized into 2c—2e chemical bonds. Second, MOs, which cannot be localized into 2c—2e bonds, are identified as σ-delocalized or π-delocalized. Third, the π-aromaticity (or π-antiaromaticity) and the σ-aromaticity (or σ-antiaromaticity) is assigned to a cluster on the basis of counting of the delocalized electrons according to the $4n + 2$ rule for aromaticity (the singlet coupling electrons) and the $4n$ rule for antiaromaticity (the singlet coupling electrons). For the triplet coupling of electrons, we use the inverse $4n$ counting rules for aromaticity. Thus in our analysis, we mix two ways of describing chemical bonding in boron clusters: localized MOs and delocalized MOs. In the result, chemical bonding is expressed in terms of 2c—2e bonds and lone pairs as well as multiple aromaticity, multiple antiaromaticity or conflicting (σ-aromaticity and π-antiaromaticity, or σ-antiaromaticity and π-aromaticity) aromaticity. Such a mixed analysis is not new in chemistry. It is constantly used in organic chemistry. For example, in benzene, σ-electrons are treated as forming localized 2c—2e C—C bonds, while π-electrons are treated as completely delocalized over six carbon atoms.

The concept of "double aromaticity" was initially introduced in 1979 by Schleyer and coworkers for explanation of chemical bonding in 3,5-didehydrophenyl cation.[75] Double aromaticity and antiaromaticity in small carbon rings was discussed by Martin-Santamaria and Rzepa.[76] ($\pi + \sigma$)-Double aromaticity and (π, σ)-mixed aromaticity have been used by Berndt and coworkers for explaining chemical bonding in planar boron compounds.[77]

B_3^+ and B_3^- Clusters

The B_3^+ cluster is a perfect triangle in the closed shell ground spectroscopic state (D_{3h}, $^1A_1'$, $1a_1'^2 1e'^4 1a_2''^2$)[35,36,39,42,49] (Fig. 1). Molecular orbital picture of four valence MOs is presented in Figure 2. The HOMO ($1a_2''$) is a π-MO, formed by the out-of-plane overlap of $2p_z$-AOs of the three B atoms. We localized the remaining set of valence MOs ($1e'$-HOMO-1 and $1a_1'$-HOMO-2) into three 2c—2e B—B bonds with the occupation numbers (ON) 1.89 |e| using NBO analysis at the B3LYP/6-311 + G* level of theory in the putative B_3^{3+} cation ($1a_1'^2 1e'^4$ electronic configuration) at the geometry of the B_3^+ cluster. The strong s–p hybridization in the B_3^{3+} cation ($2s^{0.96}2p^{1.03}$) is responsible for bonding character of the lowest three valence MOs [correction to our statement in the ref. 14a, where we stated that the bonding effect from these MOs should be small]. The two

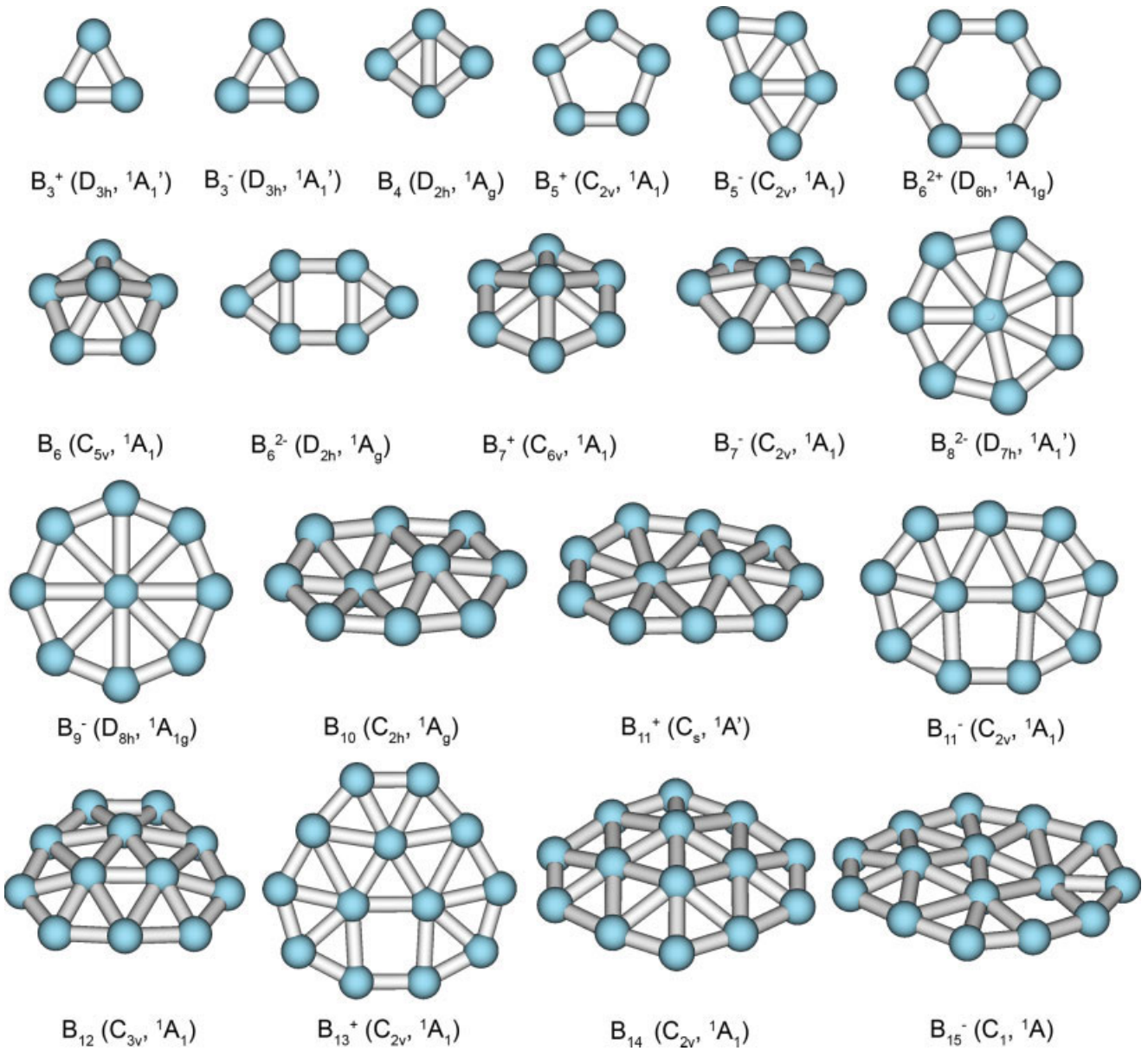

Figure 1. Global minimum structures of B_3^+, B_3^-, B_4, B_5^+, B_5^-, B_6^{2+}, B_6, B_6^{2-}, B_7^+, B_7^-, B_8^{2-}, B_9^-, B_{10}, B_{11}^+, B_{11}^-, B_{12}, B_{13}^+, B_{14}, and B_{15}^- as reported in ref. 63.

electrons in the fully delocalized π-HOMO make B_3^+ π-aromatic, obeying the $4n + 2$ Hückel rule for $n = 0$. Three other MOs represent 2c—2e bonds, even though their ON (1.89 |e|) are somewhat lower than 2.00 |e| for the classical 2c—2e bonds. Its aromatic character is confirmed by highly symmetric structure and highly negative NICS values: NICS(0) = −66.3 ppm; NICS(0.5) = −46.3 ppm, and NICS(1.0) = −15.9 ppm (Table 1). The small first singlet vertical excitation energy (0.77 eV, Table 1) reflects the presence of low-lying completely bonding σ-aromatic LUMO ($2a_1'$).

In the triangular ground electronic state of the B_3^- cluster,[14,49,55] the extra pair of electrons occupies $2a_1'$-MO (LUMO in B_3^+, Fig. 2), which is a σ-molecular orbital, formed by the radial overlap of the 2p-atomic orbitals on boron atoms (Fig. 2). The two electrons in the fully delocalized σ-HOMO make B_3^- σ-aromatic. The doubly occupied π-HOMO-1 is responsible for π-aromaticity in B_3^-. $1a_1'$ HOMO-3 and $1e'$ HOMO-2 can be transformed into three 2c—2e B—B bonds. Thus, B_3^- is a doubly (σ- and π-) aromatic system. Its doubly aromatic character is confirmed by NICS value: NICS(0) = −73.6 ppm; NICS(0.5) = −57.9 ppm; and NICS(1.0) = −28.2 ppm (Table 1). High symmetry and rather high first singlet vertical excitation energy (2.65 eV at TD-B3LYP/6-311 + G*, Table 1) also confirm the doubly-aromatic character of B_3^-.

Table 1. Computed Features of Chemical Bonding in Boron Clusters.[a]

Cluster	Number of 2c−2e B−B bonds	Number of totally delocalized σ-MOs	Number of totally delocalized π-MOs	NICS (ppm)	First singlet vertical excitation energy (eV)	E_{atomiz} (kcal/mol per atom)
B_3^+ D_{3h} ($^1A_1'$)	3	0	1	−66.3 (0.0) −46.3 (0.5) −15.9 (1.0)	0.77	56.4
B_3^- D_{3h} ($^1A_1'$)	3	1	1	−73.6 (0.0) −57.9 (0.5) −28.2 (1.0)	2.65	88.43
B_4 D_{2h} (^1A_g)	4	1	1	−35.6 (0.0) −24.5 (0.5) 7.7 (1.0)	3.08	79.65
B_5^+ D_{5h} ($^1A_1'$)	5	1	1	−36.2 (0.0) −31.0 (0.5) −18.8 (1.0)	2.97	88.04
B_5^- C_{2v} ($^1A_1$)	5	2	1	−10.8 (0.0) −16.9 (0.5) −14.3 (1.0)	1.10	98.10
B_6^{2+} D_{6h} ($^1A_{1g}$)	6	1	1	−29.6 (0.0) −26.2 (0.5) −17.8 (1.0)	1.94	70.02
B_6^0 C_{5v} ($^1A_1$)	5	3	1	−59.1 (−0.15) −41.9 (−0.65) −23.3 (−1.15)	2.34	89.18
B_6^{-2} D_{2h} (^1A_g)	6	2	2	−3.6 (0.0) 3.4 (0.5) 8.9 (1.0)	0.88	93.57
B_7^+ C_{6v} ($^1A_1$)	6	3	1	−42.3 (−0.1) −36.0 (−0.6) −20.4 (−1.1)	1.99	98.74
B_8^{2-} D_{7h} ($^1A_1'$)	7	3	3	−84.7 (0.0) −27.0 (0.5) −24.8 (1.0)	1.75	106.31
B_9^- D_{8h} ($^1A_{1g}$)	8	3	3	−28.3 (0.0) −23.3 (0.5) −13.7 (1.0)	2.79	110.62
B_{10}^0 C_{2h} (^1A_g)	9	3	3	−17.0 (0.0) −15.2 (0.5) −13.3 (1.0)	1.95	105.19
B_{11}^+ C_s ($^1A'$)	10	3	3	−19.6 (−0.0) −20.0 (−0.5) −15.3 (1.0)	1.34	108.20
B_{11}^- C_{2v} ($^1A_1$)	10	4	3	−18.5 (0.0) −20.1 (0.5) −17.0 (1.0)	1.81	114.27
B_{12}^0 C_{3v} ($^1A_1$)	12	3	3	−28.4 (−0.04) −27.1 (−0.54) −19.9 (−1.04)	2.57	107.24
B_{13}^+ C_{2v} ($^1A_1$)	13	3	3	−17.2 (0.0) −21.5 (0.5) −20.2 (1.0)	2.09	111.21
B_{14} C_{2v} ($^1A_1$)	14	3	4	−14.5 (0.6) −19.0 (0.1) −11.9 (−0.4)	1.50	108.74
B_{15}^- C_1 (^1A)	15	4	4	−11.4 (0.0) −12.0 (0.5) −8.8 (1.0)	1.02	114.5

[a]All data at B3LYP/6-311 + G*.

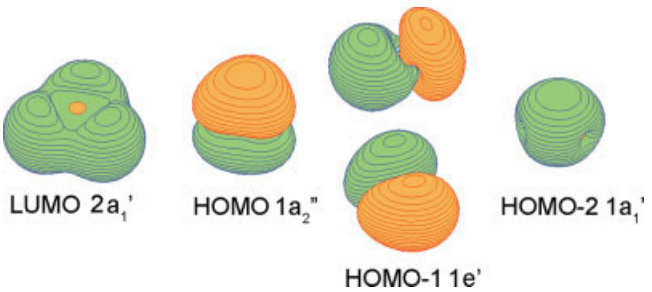

Figure 2. Molecular orbitals of the B_3^+ cation.

B_4 and B_4^{2-} Clusters

The structure of neutral B_4 was carefully studied by Martin et al.[35] They predicted the D_{2h} ^1A_g rhombus global minimum structure (see Fig. 1). Such a distortion from the perfect square comes from the second-order (or "pseudo") Jahn-Teller effect, as it was discussed by Martin et al.[35] Because of the nature of the distortion, the barrier for "squareness" is rather small (0.7–0.8 kcal/mol)[14a,58] and even at moderate temperature, the B_4 cluster is effectively square.

Molecular orbitals of the D_{2h} (^1A_g, $1a_g^2 1b_{1u}^2 1b_{2u}^2 1b_{3g}^2 1b_{3u}^2 2a_g^2$) structure of B_4 are shown in Figure 3. The lowest four MOs (HOMO-2 ($1b_{3g}$), HOMO-3 ($1b_{2u}$), HOMO-4 ($1b_{1u}$), HOMO-5 ($1a_g$)) can be localized, as it has been shown by NBO analysis, into four classical peripheral 2c—2e B—B bonds (Table 2). Again, the strong s–p hybridization on the both types of boron atoms: $2s^{0.95}2p^{1.14}$ and $2s^{1.04}2p^{0.83}$ (from HOMO-2 through HOMO-5) is responsible for the formation of four classical B—B bonds. The remaining two MOs are globally delocalized, and participate in the global bonding in the cluster. NBO analysis in this case shows eight lone pairs with the occupation number 0.5 *e* (Table 2) on each atom. The HOMO-1 ($1b_{3u}$) is a completely bonding π-molecular orbital formed by the out-of-plane overlap of $2p_z$-AOs on the B atoms. The two electrons populating this MO make the cluster π-aromatic. The HOMO ($2a_g$) of B_4 is a σ-radial molecular orbital, just like the HOMO ($2a_1'$) of B_3^-, formed by the radial overlap of 2p-AOs. The system thus can be characterized as σ-aromatic, i.e., B_4 is a doubly-aromatic molecule as it was first recognized by Zhai et al.[14a] This conclusion is supported by effective high symmetric (square) structure, calculated the first singlet vertical excitation energy (3.08 eV X $^1A_g \rightarrow A$ $^1B_{3g}$ at TD-B3LYP/6-311 + G*, Table 1) and calculated NICS index, which is highly negative at the center of the cluster (−35.7 ppm), but quickly diminishes and changes the sign at 1.0 A above the center (+7.7 ppm) (Table 1).

The doubly charged B_4^{2-} cluster has a square planar D_{4h} $^1A_{1g}$ ($1a_{1g}^2 1e_u^4 1b_{1g}^2 1b_{2g}^2 2a_{1g}^2 1a_{2u}^2$) structure according to Sundholm and coworkers,[8a] who used the isoelectronic analogy with Al_4^{2-}, where extensive search for the global minimum structure has been performed,[1a,1b] and the D_{4h} $^1A_{1g}$ square planar structure was found to be the most stable isomer. The Al_4^{2-} dianion has been studied extensively and it was shown using a variety of criteria that it is a doubly (σ- and π-) aromatic system [1a and references therein]. Thus, the isoelectronic, isostructural B_4^{2-} is also doubly (σ- and π-) aromatic system with four 2c—2e peripheral B—B bonds. Sundholm and coworkers[8a] also confirmed aromaticity in B_4^{2-} by calculating the ring-current susceptibility, which was found to be 7.4 nAT^{-1}. That is only 10% smaller than that for the value of the prototypical aromatic benzene molecule, thus confirming the aromatic nature of the dianion.

B_5^+ and B_5^- Clusters

Kato et al.[36] and Rica and Bauschlicher[42] reported that in the global minimum, B_5^+ adopts the C_{2v} structure, which is a slightly distorted planar pentagon. Rica and Bauschlicher stated that the D_{5h} ($^1A_1'$,$1a_1'^2 1e_1'^4 1e_2'^4 1a_2''^2 2a_1'^2$) planar pentagon has two imaginary frequencies at the B3LYP/cc-pvTZ level of theory and in the global minimum, C_{2v} ($^1A_1$, $1a_1^2 1b_2^2 2a_1^2 3a_1^2 1b_1^2 2b_2^2 4a_1^2 3b_2^2$) structure B—B bonds are only slightly distorted. This distortion is due to the second order Jahn-Teller Effect. According to our calculations (CCSD(T)/6-311 + G*), the global minimum C_{2v} ($^1A_1$) structure (Fig. 1) is only 0.365 kcal/mol lower in energy than the second-order saddle point D_{5h} ($^1A_1'$) planar pentagon structure and after ZPE correction (harmonic frequencies at CCSD(T)/6-311 + G*), the vibrationally averaged D_{5h} ($^1A_1'$) structure is actually lower in energy than the vibrationally averaged C_{2v} ($^1A_1$) structure by 0.010 kcal/mol. Thus, for all practical purposes, we can consider the B_5^+ cluster as a planar pentagon.

The beautiful planar pentagonal structure of B_5^+ can be understood from its molecular orbital analysis (Fig. 4). The NBO analysis showed that HOMO-2 and HOMO-2′ ($1e_2'$), HOMO-3 and HOMO-3′ ($1e_1'$), and HOMO-4 ($1a_1'$) can be localized into five peripheral 2c—2e B—B bonds. The HOMO ($2a_1'$) in B_5^+ is a globally bonding σ-MO, and HOMO-1 ($1a_2''$) is a globally bonding π-MO. Thus, they make the cation doubly (σ- and π-) aromatic. Double aromaticity in conjunction with the presence of five 2c—2e B—B peripheral bonds is responsible for the vibrationally averaged highly symmetry D_{5h} structure of the B_5^+ cluster. Also, double aromaticity in B_5^+ manifests itself in the high first singlet vertical excitation energy (2.97 eV at TD-B3LYP/6-311 + G*, Table 1), highly negative values of NICS: NICS(0) = −36.2 ppm; NICS(0.5) = −31.0 ppm, and

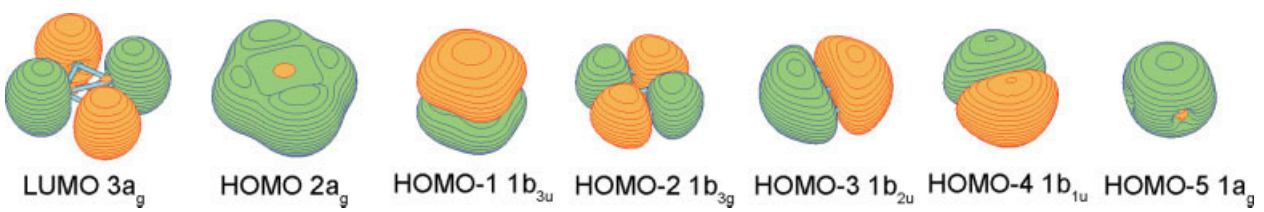

Figure 3. Molecular orbitals of the B_4 cluster.

Table 2. Localized MOs[a] of the D_{2h}, ^1A_g Structure of B_4.

LMO type	Occupation number |e|	Composition
B_1–B_2	1.977	50.49% B_1: 2s – 47.79%; 2p – 52.03% 49.51% B_2: 2s – 49.93%; 2p – 49.91%
B_1–B_3	1.977	50.49% B_1: 2s – 47.79%; 2p – 52.03% 49.51% B_3: 2s – 49.93%; 2p – 49.91%
B_2–B_4	1.977	49.51% B_2: 2s – 49.93%; 2p – 49.91% 50.49% B_4: 2s – 47.79%; 2p – 52.03%
B_3–B_4	1.977	49.51% B_3: 2s – 49.93%; 2p – 49.91% 50.49% B_4: 2s – 47.79%; 2p – 52.03%
Lone pair B_1	0.576	B_1: 2s – 0.0%; 2p – 99.5%
Lone pair B_1	0.529	B_1: 2s – 5.1%; 2p – 93.9%
Lone pair B_4	0.576	B_4: 2s – 0.0%; 2p – 99.5%
Lone pair B_4	0.529	B_4: 2s – 5.1%; 2p – 93.9%
Lone pair B_2	0.503	B_2: 2s – 1.6%; 2p – 97.7%
Lone pair B_2	0.424	B_2: 2s – 0.0%; 2p – 99.6%
Lone pair B_3	0.503	B_3: 2s – 1.6%; 2p – 97.7%
Lone pair B_3	0.424	B_3: 2s – 0.0%; 2p – 99.6%

[a]LMO calculated at B3LYP/6-311 + G* using the NBO analysis.

NICS(1.0) = −18.8 ppm (Table 1) and most importantly it explains why B_5^+ is a magic cluster in collision induced dissociation (CID) experiments by Anderson and coworkers.[23–31] The distortion of the D_{5h} ($^1A_1'$) structure can be explained by the second-order Jahn-Teller effect, because there is nothing in occupied MOs (Fig. 4) of the pentagon indicating the deviation from high symmetry. That case is similar to the distortion of the B_4 cluster into rhombus and like in that case the second-order distortion makes the B_5^+ potential energy surface very shallow.

For the B_5^- cluster, we can predict the global minimum structure if we start with the B_5^+ cluster. The $1e_1''$-LUMO in B_5^+ D_{5h} ($^1A_1'$) is a doubly degenerate π-MO, which is a partially bonding/antibonding orbital related to the completely bonding $1a_2''$-HOMO-1 π-MO. These three MOs are a part of the set of 5 MOs formed by the $2p_z$-AOs of B and responsible for global π-bonding. Occupation of one of doubly degenerate LUMO by two electrons should lead to distortion of the D_{5h} structure to the C_{2v} structure because of the first order Jan-Teller effect. Our calculations have shown that the resulting C_{2v} ($^1A_1$, $1a_1^2 1b_2^2 2a_1^2 3a_1^2 1b_1^2 2b_2^2 4a_1^2 1a_2^2$) structure is 50.6 (B3LYP/6-311 + G*) kcal/mol higher than the global minimum and it is a first order saddle point. Geometry optimization following the imaginary frequency normal mode led eventually to the global minimum structure.

In the global minimum structure, the LUMO +1 ($2e_1'$-MO) is partially occupied instead of LUMO ($1e_1''$). The singlet $1a_1'^2 1e_1'^4 1e_2'^4 1a_2''^2 2a_1'^2 1e_1''2$ electronic configuration of the D_{5h} structure of B_5^- should also lead to the first order Jahn-Teller distortion. Indeed, it was shown that the C_{2v} ($^1A_1$, $1a_1^2 1b_2^2 2a_1^2 3a_1^2 1b_1^2 2b_2^2 4a_1^2 3b_2^2$) planar structure is the B_5^- global minimum structure. The LUMO +1 in B_5^+ belongs to a partially bonding/antibonding σ-orbital related to the completely bonding σ-HOMO ($2a_1'$). These three MOs are a part of the set of 5 MOs formed by the 2p-radial AOs of B and responsible for global σ-bonding. Thus, B_5^- has four electrons on globally σ-delocalized HOMO-1 ($4a_1$) and HOMO ($3b_2$) and two electrons on globally delocalized HOMO-3 ($1b_1$), which makes B_5^- a system with conflicting aromaticity (σ-antiaromatic and π-aromatic). NBO analysis for the B_5^{5+} cation at the geometry of B_5^- and with the $1a_1^2 1b_2^2 2a_1^2 3a_1^2 2b_2^2$ electronic configuration shows that there are five 2c—2e B—B peripheral bonds (ON = 1.76–1.91 |e|). The C_{2v} $^1A_1$ structure of B_5^- has been experimentally established in joint photoelectron and *ab initio* study by Zhai et al.[15] Because the geometric structure of σ-antiaromatic and π-aromatic B_5^- anion has lower symmetry, we believe that antiaromaticity overwhelms aromaticity in this case and we prefer to call this cluster "net antiaromatic". The low first singlet vertical excitation energy (1.10 eV, at TD-B3LYP/6-311 + G*) provides us additional support in our overall assignment of aromaticity in spite of negative values of NICS in this case (Table 1). The B_5^- anion is a remarkable example showing that if we would limit our chemical bonding analysis to π-electrons only, we will not be able to explain why π-aromatic (2 π-electrons) B_5^- cluster has low C_{2v} symmetry and low first singlet vertical excitation energy.

B_6^{2+}, B_6, and B_6^{2-} Clusters

The six-atomic cyclic analog of the B_5^+ cluster should be the B_6^{2+} dication. It has 16 valence electrons and assuming the formation of six peripheral 2c—2e B—B bonds out of HOMO-2 ($1b_{2u}$), HOMO-3 and HOMO-3′ ($1e_{2g}$), HOMO-4 and HOMO-4′($1e_{1u}$), and HOMO-5 ($1a_{1g}$), we should have four electrons on two completely bonding σ-HOMO ($2a_{1g}$) and π-HOMO-1 ($1a_{2u}$) (Fig. 5a). This makes the B_6^{2+} dication doubly aromatic. Our cal-

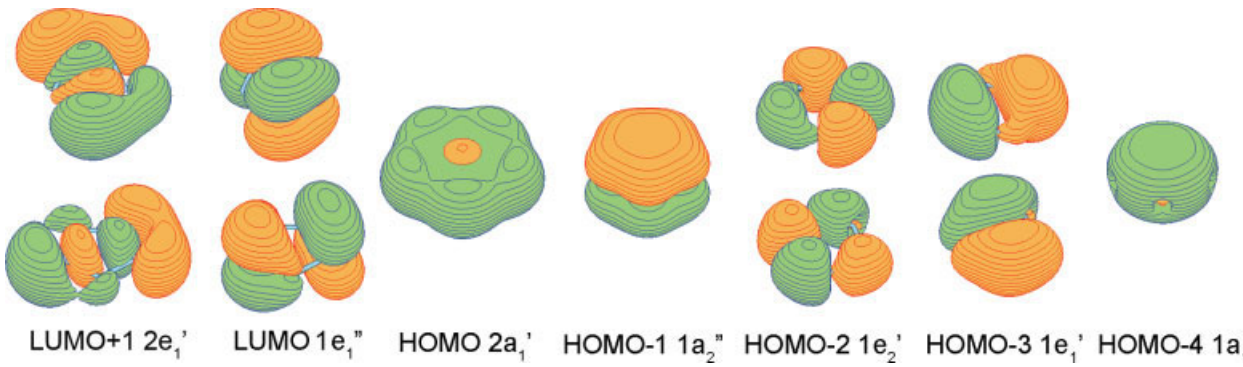

Figure 4. Molecular orbitals of the B_5^+ cation.

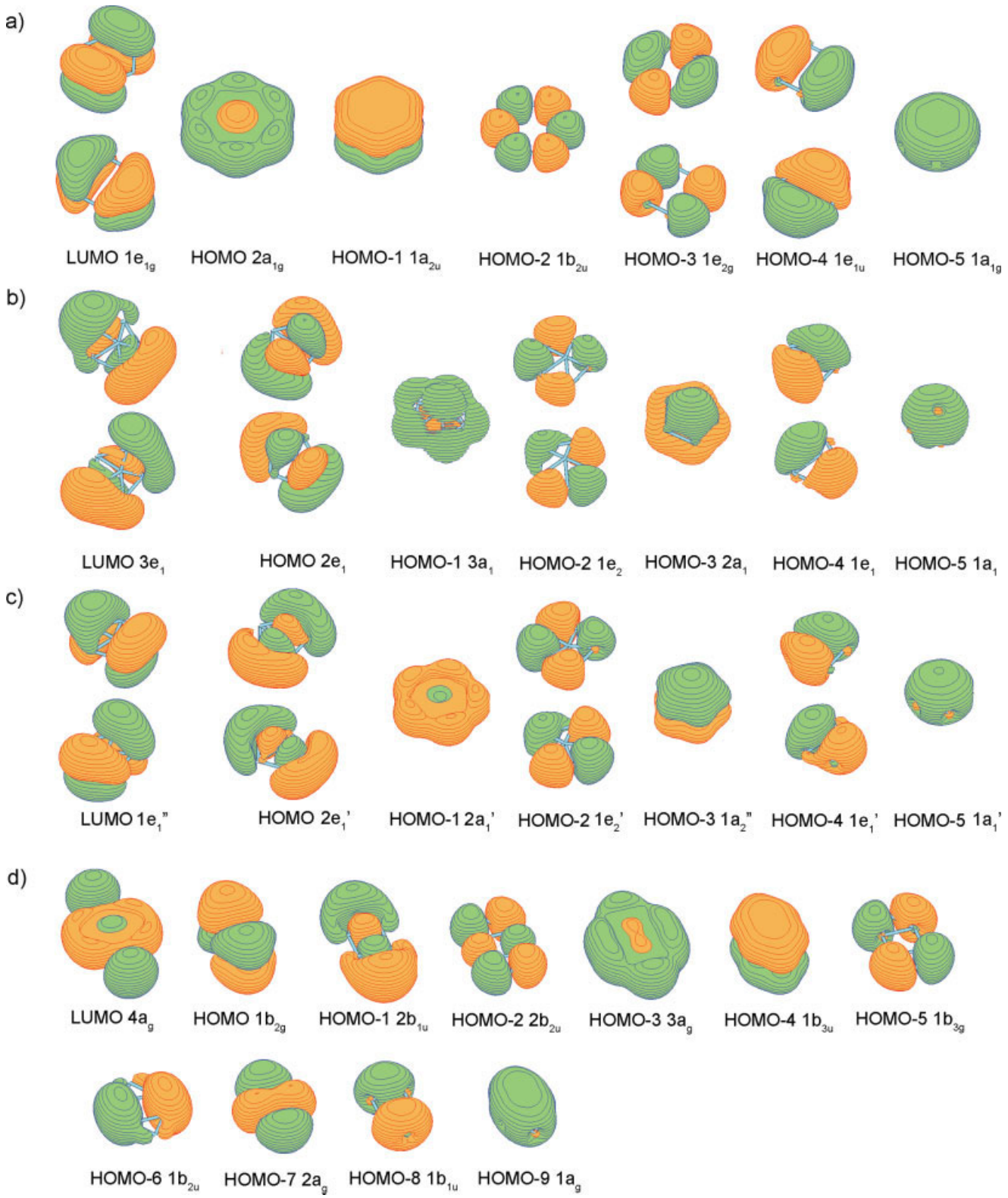

Figure 5. (a) Molecular orbitals of the D_{6h} ($^1A_{1g}$) structure of the B_6^{2+} cluster; (b) molecular orbitals of the C_{5v} ($^1A_1$) structure of the B_6 cluster; (c) molecular orbitals of the D_{5h} ($^1A_1'$) structure of the B_6 cluster; (d) molecular orbitals of the D_{2h} (^1A_g) structure of the B_6^{2-} dianion.

culations proved that the B_6^{2+} D_{6h} ($^1A_{1g}$) structure indeed is a minimum at three levels of theory (B3LYP/6-311 + G*, MP2/6-311 + G*, and CCSD(T)/6-311 + G*).

In the B_6 cluster, in addition to cyclic structures, we observe the emergence of a new type of structure—pentagonal pyramid, which now corresponds to the global minimum.[16] The planar pentagonal structure with the boron atom located at the center of the five-atomic ring is not a minimum because the cavity inside of the pentagon is too small to favorably accommodate a boron atom at the center. However, as we will see in the large boron clusters (B_8 and B_9^-), with the increase of the size of the central cavity, a boron atom can be favorably accommodated at the center of the appropriate polygon leading to planar highly symmetric global minimum structures. The most accurate calculations[16] reveal that the global minimum structure of B_6 is the pyramid C_{5v} ($^1A_1$, $1a_1^2 1e_1^4 2a_1^2 1e_2^4 3a_1^2 2e_1^4$) structure with the boron atom located 0.94 Å above the center of the B_5 perfect pentagon. The triplet C_{2h} ^3A_u ($1a_g^2 1b_u^2 2a_g^2 2b_u^2 3a_g^2 1a_u^2 3b_u^2 4a_g^2 4b_u^1 1b_g^1$) and the singlet C_2 ^1A ($1a^2 1b^2 2b^2 2a^2 3a^2 4a^2 3b^2 5a^2 4b^2$) structures originating from the cyclic B_6 geometry upon Jahn-Teller distortions were found to be 7.2 and 8.2 kcal/mol (CCSD(T)/6-311 + G(2df)//B3LYP/6-311 + G*), respectively, higher in energy.[16]

To simplify interpretation of molecular orbitals, let us first perform MO analysis for the D_{5h} ($^1A_1'$, $1a_1'^2 1e_1'^4 1a_2'' 1e_2'^2 2a_1'^2 2e_1'4$) structure (Fig. 5c), in which the central atom is pushed into the center. The set of five MOs (HOMO-2 and HOMO-2′ ($1e_2'$), HOMO-4, and HOMO-4′ ($1e_1'$), and HOMO-5 ($1a_1'$)) can be localized into five 2c—2e B—B bonds, so they are responsible for the peripheral bonding. The HOMO-3 ($1a_2''$) is formed by $2p_z$-AOs, and it is responsible for the global π-bonding. The HOMO and HOMO′ ($2e_1'$), and HOMO-1 ($2a_1'$) are formed from 2p-radial AOs, and they are responsible for global σ-bonding in the B_6 cluster. Thus, B_6 in the D_{5h} $^1A_1'$ configuration is a doubly (σ- and π-) aromatic system with 2π- and 6σ-electrons. However, as we mentioned above, the central cavity in the B_5 pentagon is too small to favorably accommodate the central boron atom, and therefore a C_{5v} $^1A_1$ pyramidal structure corresponds to the global minimum. While in the pyramidal structure σ- and π-MOs are mixed, we believe that the bonding picture developed for the D_{5h} $^1A_1'$ structure is still qualitatively valid and can explain why B_6 clusters adopts such a structure.

When two extra electrons are added, the planar D_{2h} ^1A_g ($1a_g^2 1b_{1u}^2 2a_g^2 1b_{2u}^2 1b_{3g}^2 1b_{3u}^2 3a_g^2 2b_{2u}^2 2b_{1u}^2 1b_{2g}^2$) structure becomes the global minimum for the B_6^{2-} dianion.[7b,16] This structure is originating from the D_{6h} hexagon, which underwent the first order Jahn-Teller distortion. Molecular orbital analysis helps us to interpret chemical bonding in B_6^{2-} (Fig. 5d). Six MOs (HOMO-2 ($2b_{2u}$), HOMO-5 ($1b_{3g}$), HOMO-6 ($1b_{2u}$), HOMO-7 ($2a_g$), HOMO-8 ($1b_{1u}$), and HOMO-9 ($1a_g$)) can be localized into six 2c—2e B—B bonds, so they are responsible for the peripheral bonding in this cluster. The remaining four MOs are responsible for the global bonding in the B_6^{2-} cluster. The HOMO-1 ($2b_{1u}$) and HOMO-3 ($3a_g$) are σ-radial MOs, with the HOMO-3 being completely bonding, and the HOMO-1 being partially antibonding. Thus, B_6^{2-} has two globally delocalized σ-MOs, which makes this dianion σ-antiaromatic. The two other delocalized orbitals HOMO-4 ($1b_{3u}$) and HOMO ($1b_{2g}$) are π-MOs. The HOMO-4 is completely bonding, and the HOMO is a partially bonding orbital. The B_6^{2-} dianion has 4 σ- and 4 π-electrons on the globally delocalized MOs and six 2c—2e peripheral B—B bonds. Thus, we can assign B_6^{2-} to doubly (σ- and π-) antiaromatic systems. The question may arise, why a doubly antiaromatic structure is the global minimum. We believe that this is because the B_6^{2-} cannot favorably support six delocalized electrons in either σ- or π-subsystems. Electrostatic field from the screened boron nuclei does not provide enough stabilization for six electrons in either σ- and π-subsystems and that leads to a compromised globally doubly antiaromatic structure.

In a recent article, Aihara et al.[20] claimed that the boron B_6^{2-} cluster is highly aromatic on the basis of topological resonance energy (TRE). The calculated TRE for B_6^{2-} in terms of the resonance integral between two bonded boron atoms ($|\beta_{BB}|$) is 0.549 $|\beta_{BB}|$. This value expressed in terms of the resonance integral between two bonded carbon atoms ($|\beta_{CC}|$) is 0.478 $|\beta_{CC}|$. For the reference, the TRE for benzene is 0.273 $|\beta_{CC}|$. Thus, according to Aihara et al.,[20] the B_6^{2-} cluster is clearly showing the presence of aromaticity. However, this large resonance energy does not contradict our assignment of B_6^{2-} to doubly antiaromatic systems. Our assignment of B_6^{2-} to π-antiaromatic system is based on the presence of 4 π-electrons, its highly distorted (D_{2h}) structure, and paratropic ring currents calculated by Fowler and coworkers (see ref. 16 for details). We see this cluster as being antiaromatic globally. It does not, however, mean that this cluster cannot have positive resonance energy. In fact, according to our MO analysis, we can consider the π-system in B_6^{2-} as being split into two subsystems, with two π-electrons localized over each of two triangular regions. π-MOs of B_6^{2-} cluster can be viewed as composed of two aromatic B_3^- clusters (see ref. 16 for detailed discussion). Indeed, $1b_{2g}$-HOMO and $1b_{3u}$-HOMO-4 are a pair of bonding and antibonding π-MOs in B_3^-. Thus, π-MOs do not contribute significantly to chemical bonding between two B_3^- groups. This allows us to speculate that π-MOs in B_6^{2-} give rise to an island π-aromaticity in this cluster. Similar analysis for the delocalized σ-MOs reveals that we also have an island σ-aromaticity in B_6^{2-}. Thus, the globally antiaromatic B_6^{2-} system can be considered as having two island aromatic subunits. The island π-aromaticity is responsible for positive TRE in B_6^{2-} in Aihara et al.[20] calculations. Indeed, Aihara et al.[20] stated that three (a2–a4) out of four circuit currents (Fig. 6) are paratropic indicating antiaromaticity and the a1 circuit current, which is located over triangular region, is highly diatropic. It overwhelms the antiaromatic con-

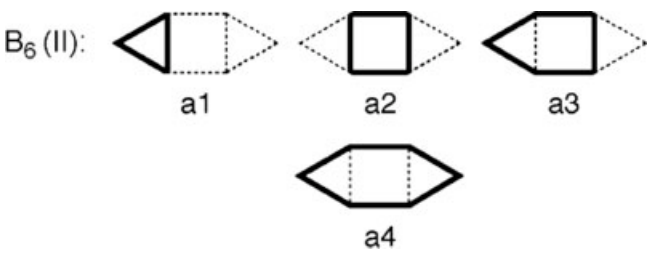

Figure 6. Nonidentical circuits in B_6^{2-} (adopted from ref. 20).

tributions from the a2a–4 a1 circuit currents and results in the overall positive TRE. This result clearly supports the presence of island aromaticity in B_6^{2-}. Alexandrova et al.[22] have shown that for Li_2B_6 molecule in the gas phase, the global minimum structure is C_{2h} ($^1A_1$) with two Li^+ ions located above and below the B_3^- triangular areas in B_6^{2-}. The D_{2h} (^1A_g) structure, containing one Li^+ cation above and another Li^+ below the plane of B_6^{2-} dianion, was found to be a saddle point on the potential energy surface. These results confirmed the presence of the π-island aromaticity in the globally antiaromatic system.

B_7^+ and B_7^- Clusters

The global minimum structure of the cationic B_7^+ cluster is the C_{6v} $^1A_1$ ($1a_1^2 1e_1^4 1e_2^4 2a_1^2 1b_1^2 3a_1^2 2e_1^4$) pyramid[36,39,41,55,60] with the central boron atom located 0.72 Å above the plane (Fig. 1). To simplify the interpretation of the molecular orbitals, we performed MO analysis of the D_{6h} ($^1A_{1g}$, $1a_{1g}^2 1e_{1u}^4 1e_{2g}^4 1b_{2u}^2 2a_{1g}^2 1a_{2u}^2 2e_{1u}^4$) structure (Fig. 7b), in which the central atom is pushed into the plane. The set of six MOs (HOMO-3 ($1b_{2u}$), HOMO-4 and HOMO-4′ ($1e_{2g}$), HOMO-5, and HOMO-5′ ($1e_{1u}$) and HOMO-6 ($1a_{1g}$)) is responsible for the peripheral bonding and can be localized into six 2c—2e B—B bonds. The HOMO-1 ($1a_{2u}$) is formed by $2p_z$-AOs and is responsible for the global π-bonding. The HOMO and HOMO′ ($2e_{1u}$), and HOMO-2 ($2a_{1g}$) are formed from 2p-radial AOs and they are responsible for global σ-bonding in the B_7^+ cluster. Thus, B_7^+ in the D_{6h} $^1A_{1g}$ configuration is doubly (σ- and π-) aromatic system with 2π- and 6σ-electrons. However, the central cavity in the B_6 hexagon is too small to favorably accommodate the central boron atom, and therefore, the C_{6v} $^1A_1$ pyramidal structure corresponds to the global minimum. While in the pyramidal C_{6v} $^1A_1$ structure σ- and π-MOs are now mixed, we believe that the bonding picture we developed for the D_{6h} $^1A_{1g}$ structure is still qualitatively valid.

The seven-atomic cyclic structure of the B_7^+ cluster is a local minimum with the $^3A_2'$ ($1a_1'^2 1e_1'^4 1e_2'^4 1e_3'^4 1a_2''^2 2a_1'^2 1e_1''^2$) spectroscopic state. It has 20 valence electrons and assuming the formation of seven peripheral 2c—2e B—B bonds from HOMO-3 and HOMO-3′ ($1e_3'$), HOMO-4 and HOMO-4′($1e_2'$), HOMO-5 and HOMO-5′ ($1e_1'$) and HOMO-6 ($1a_1'$), we should have six electrons for global bonding. Two of them occupy the completely bonding σ-HOMO-1 ($2a_1'$). Two electrons occupy the completely bonding π-HOMO-2 ($1a_2''$) and two electrons occupy the partially bonding doubly degenerate π-HOMO ($1e_1''$) with the triplet coupling. This makes the B_7^+ dication doubly aromatic in the cyclic structure. However, the B_7^+ D_{7h} ($^3A_2'$) structure is significantly higher (63.4 kcal/mol at B3LYP/6-311 + G*) in energy than the global minimum C_{6v} ($^1A_1'$) structure, because of unsupported dangling electron density at the center of the cycle. Thus, the cyclic structures are not favorable anymore beyond six boron atoms.

According to the Alexandrova et al.[17] calculations, the B_7^- cluster has a very flat triplet C_{6v} $^3A_2$ ($1a_1^2 1e_1^4 1e_2^4 2a_1^2 3a_1^2 1b_1^2 2e_1^4 3e_1^2$)[78] pyramidal structure similar to the B_7^+ structure as the global minimum. The second lowest C_{2v} $^1A_1$ ($1a_1^2 1b_2^2 1b_1^2$ $2a_1^2 1a_2^2 3a_1^2 2b_1^2 4a_1^2$ $2b_2^2 3b_1^2 3b_2^2$) structure (Fig. 1) was found to be just 0.7 kcal/mol higher (RCCSD(T)/6-311+G(2df)//RCCSD(T)/6-311 + G*) in energy than the global minimum structure. Thus, these two structures are almost degenerate. The combined photoelectron spectroscopic and *ab initio* study[17] suggests that at least two isomers C_{6v} $^3A_2$ and C_{2v} $^1A_1$ could coexist in the B_7^- beam and contribute to the photoelectron spectra of B_7^-.

MO analysis was performed for the planar B_7^- D_{6h} $^3A_{2g}$ ($1a_{1g}^2 1e_{1u}^4 1e_{2g}^4 1b_{2u}^2 2a_{1g}^2 1a_{2u}^2 2e_{1u}^4 1e_{1g}^2$) (In ref. 17 the $^3A_1$ spectroscopic state was reported for the $1a_1^2 1e_1^4 1e_2^4 2a_1^2 3a_1^2 1b_1^2 2e_1^4 3e_1^2$ electronic configuration of the B_7^- C_{6v} structure as determined by the Gaussian 03 program. However, the correct spectroscopic state for such electronic configuration is $^3A_2$. Similarly, in ref. 17 the $^3A_{1g}$ was reported for the $1a_{1g}^2 1e_{1u}^4 1e_{2g}^4 1b_{2u}^2 2a_{1g}^2 1a_{2u}^2 2e_{1u}^4 1e_{1g}^2$ configuration of the B_7^- D_{6h} structure, while the correct spectroscopic state is $^3A_{2g}$) model system. NBO analysis showed that the set of low-energy MOs (Fig. 7b): HOMO-7 ($1a_{1g}$), HOMO-6 and HOMO-6′ ($1e_{1u}$), HOMO-5 and HOMO-5′ ($1e_{2g}$) and HOMO-3 ($1b_{2u}$) can be localized into six peripheral 2c—2e B—B bonds, forming the hexagonal framework. HOMO-2 ($1a_{2u}$), which is a completely bonding π-MO and partially antibonding and partially occupied HOMO, and HOMO′ ($1e_{1g}$) make this cluster π-aromatic with 4 π-electrons according to the inverse $4n$ rule for triplet states. HOMO-3 ($2a_{1g}$) and HOMO-1 and HOMO-1′ ($2e_{1u}$) are delocalized σ-MOs, which make this cluster σ-aromatic. Thus, the B_7^- cluster is a doubly (σ- and π-) aromatic system with six peripheral B—B bonds.

B_8, B_8^{2-}, and B_9^- Clusters

The neutral B_8 cluster has a triplet perfect heptagon structure D_{7h} $^3A_2'$ ($1a_1'^2 1e_1'^4 1e_2'^4 2a_1'^2 1e_3'^4 1a_2''^2 2e_1'^4 1e_1''^2$) in its ground electronic state (correction to the previous statement in ref. 18) as it was established by Zhai et al.[18] Another wheel-type structure C_s $^1A'$ was identified as a low-lying isomer.[18] The C_s $^1A'$ isomer is a Jahn-Teller distorted heptagon, because in the heptagon singlet structure only one out of two doubly degenerate $1e_1''$-HOMOs is occupied.

In the triplet D_{7h} $^3A_2'$, perfect heptagon structure HOMO-3 and HOMO-3′ ($1e_3'$), HOMO-5 and HOMO-5′ ($1e_2'$), HOMO-6 and HOMO-6′ ($1e_1'$), and HOMO-7 ($1a_1'$) (Fig. 8) can be localized into seven 2c—2e B—B bonds, HOMO and HOMO′ ($1e_1''$), and HOMO-2 ($1a_2''$) (Fig. 8) are formed from $2p_z$-AOs, and they are responsible for the global π-bonding. The HOMO-1 and HOMO-1′ ($2e_1'$) and HOMO-4 ($2a_1'$) are formed from 2p-radial AOs, and they are responsible for global σ-bonding in the B_8 cluster. Thus, the D_{7h} $^3A_2'$ structure is a doubly (σ- and π-) aromatic system with 4 π-electron (satisfying the inverse rule $4n$ rule for aromaticity for triplet coupled electrons), with 6 σ-electrons (satisfying the $4n + 2$ rule for aromaticity for singlet coupled electrons), and with seven 2c–2e peripheral B—B bonds.

In the singlet C_s $^1A'$ isomer, one of the doubly degenerate HOMOs is now occupied by a pair of electrons with another one being empty, which results in the Jahn-Teller distortion. This system is the one with conflicting aromaticity: there are 4 π-electron (satisfying $4n$ rule for antiaromaticity for a singlet coupled electrons) and 6 σ-electrons (satisfying $4n + 2$ rule for aromaticity for a singlet coupled electrons), and seven 2c–2e peripheral B—B bonds.

We also optimized the cyclic B_8 (D_{8h}, $^5A_1'$, $1a_{1g}^2 1e_{1u}^4 1e_{2g}^4 1e_{3u}^4 2a_{1g}^2 1b_{2g}^2 1a_{2u}^2 2e_{1u}^2 1e_{1g}^2$) doubly aromatic structure and found

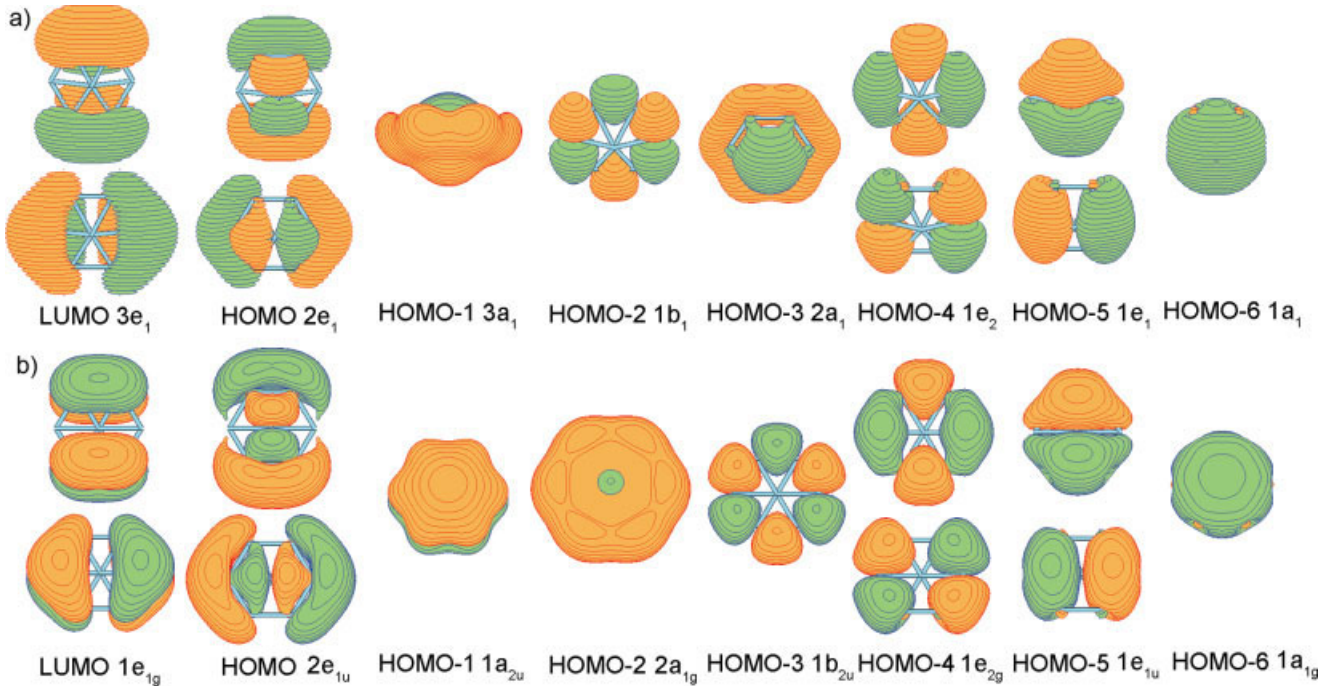

Figure 7. (a) Molecular orbitals of the C_{6v} ($^1A_1$) structure of the B_7^+ cluster; (b) molecular orbitals of the D_{6h} ($^1A_{1g}$) structure of the B_7^+ cluster.

that it is a local minimum at B3LYP/6-311 + G*. However, it is about 98 kcal/mol higher in energy than the boron-centered B_8 (D_{7h}, $^3A_2'$) doubly aromatic global minimum structure.

Thus, the cyclic structures even being doubly aromatic and corresponding to local minima are getting less and less stable with the increase of the size of the cluster starting from B_7^+ and cannot be considered even as low-energy isomers.

The doubly-charged B_8^{2-} anion has a planar D_{7h} $^1A_1'$ ($1a_1'^2 1e_1'^4 1e_2'^4 2a_1'^2 1e_3'^4 1a_2''^2 2e_1'^4 1e_1''^4$) singlet global minimum structure (Fig. 1), in which high symmetry is restored again because the doubly degenerate $1e_1''$-HOMO is now occupied by four electrons (Fig. 8). While isolated dianion was not studied experimentally, its high-symmetric structure was experimentally confirmed in a joint photoelectron spectroscopy and *ab initio* calculations of the LiB_8^- cluster by Alexandrova et al.[21] It was shown that calculated photoelectron spectrum of the half-sandwich structure of LiB_8^- in which Li^+ cation is located above the slightly distorted B_8^{2-} heptagon agrees well with the experimentally recorded spectra of the anion.

The singlet D_{7h} $^1A_1'$ structure of B_8^{2-} is a doubly (σ- and π-) aromatic system with 6 π-electron, 6 σ-electrons, and 7 2c—2e peripheral B—B bonds. This analysis of chemical bonding for B_8^{2-} was first proposed by Zhai et al.[18] Its double aromaticity is also confirmed by very high values of NICS: NICS(0) = −84.7 ppm, NICS(0.5) = −27.0 ppm, and NICS(1.0) = −24.8 ppm (Table 1).

The anionic B_9^- has the perfect planar D_{8h} ($^1A_{1g}$, $1a_{1g}^2 1e_{1u}^4 1e_{2g}^4 1e_{3u}^4 2a_{1g}^2 1b_{2g}^2 1a_{2u}^2 2e_{1u}^4 1e_{1g}^4$) wheel-shaped structure as the global minimum (Fig. 1), which was established in a joint photoelectron and *ab initio* study by Zhai et al.[18] The perfect octagon structure of B_9^- is unprecedented in chemistry and represents the first example of octacoordinated atom in a planar environment.

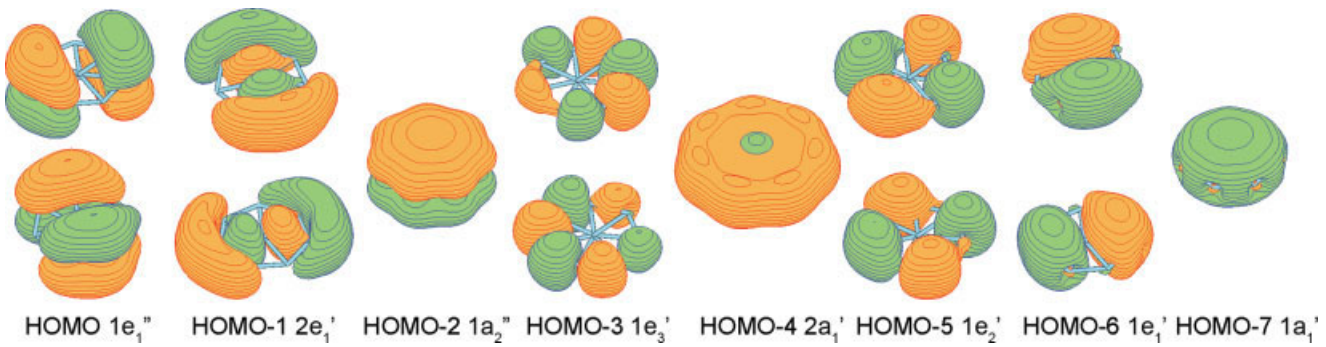

Figure 8. Molecular orbitals of the D_{7h} ($^1A_1'$) structure of the B_8^{2-} dianion.

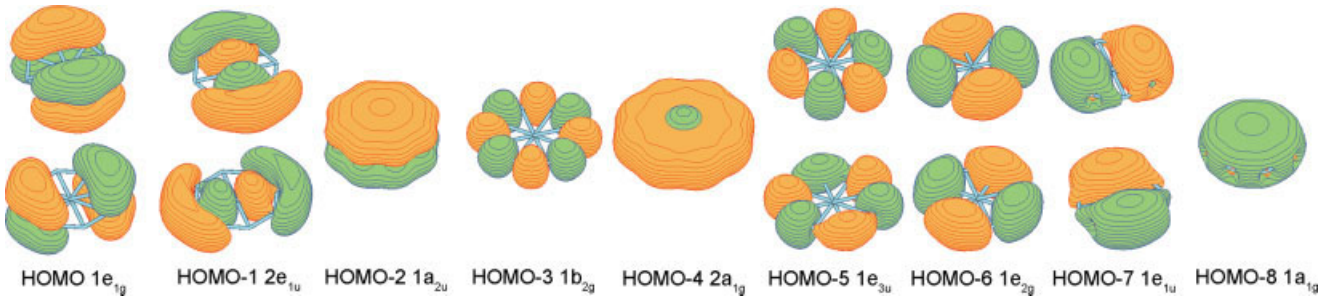

Figure 9. Molecular orbitals of the D_{8h} ($^1A_{1g}$) structure of the B_9^- anion.

The remarkable planar octagon structure of B_9^- can be easily rationalized on the basis of the presence of double (σ- and π-) aromaticity (Fig. 9).

Chemical bonding in B_9^- is remarkably similar to bonding pattern in B_8^{2-}. As before, eight MOs (Fig. 9): HOMO-3 ($1b_{2g}$), HOMO-5, HOMO-5′ ($1e_{3u}$), HOMO-6, HOMO-6′ ($1e_{2g}$), HOMO-7, HOMO-7′ ($1e_{1u}$), and HOMO-8 ($1a_{1g}$) can be localized into 8 2c—2e B—B peripheral bonds. The other valence MOs are delocalized over the octagon and they are responsible for global bonding between the central B atom and peripheral B atoms. The three π-MOs: HOMO, HOMO′ ($1e_{1g}$), and HOMO-2 ($1a_{2u}$) are responsible for π-aromaticity and the three σ-MOs: HOMO-1, HOMO-1′ ($2e_{1u}$), and HOMO-4 ($2a_{1g}$) are responsible for σ-aromaticity in B_9^-. Again, such chemical bonding analysis for B_9^- was first proposed by Zhai et al.[18] The double (σ- and π-) aromaticity in B_9^- is supported by high symmetry, high first singlet vertical excitation energy (2.79 eV at TD-B3LYP/6-311 + G*), and highly negative NICS values: NICS(0) = −28.3 ppm, NICS(0.5) = −23.3 ppm, and NICS(1.0) = −13.7 ppm (Table 1).

In addition to the wheel planar structure of B_9^-, Minkin and coworkers[78,79] reported planar structures and π-aromatic character in the CB_8, SiB_8, and PB_8^+ species. The authors found, however, that in the case of octacoordinated carbon, the central cavity is now too big to be stabilized through the accommodation of only one carbon nucleus. The D_{8h} structure of CB_8 is a second-order saddle point. The normal mode displacements lead to a C_{2v} ($^1A_1$) structure, in which the central C-atom is shifted to the side. However, the barrier on the intramolecular rearrangement is rather small and it allows one to consider the fluxional CB_8 system as one with the effective octacoordination of the central atom. The two other SiB_8 and PB_8^+ clusters were found to have a perfect octagonal structure. We would like to stress that on the basis of our analysis of chemical bonding in B_9^-, the valence isoelectronic CB_8, SiB_8, and PB_8^+ species are also σ-aromatic with six σ-electrons and they also have eight 2c—2e peripheral B—B bonds. π- and σ-aromaticity together with eight peripheral B—B bonds are responsible for the beautiful octagonal structure of these species.

B_{10}, B_{11}^+, and B_{11}^- Clusters

The B_{10}, B_{11}^+, and B_{11}^- clusters in their global minimum structures (Fig. 1) have a common feature—two boron atoms located inside either eight- (B_{10}) or nine- (B_{11}^+ and B_{11}^-) membered ring. Therefore, we will consider chemical bonding in these clusters together.

The global minimum of B_{10} according to Zhai et al.[19] and Boustani[44] is the C_{2h}, ^1A_g structure (Fig. 1), which is nonplanar with eight boron atoms forming a planar cycle around two atoms at the center, with one of the central atoms located above the plane and the other one below the plane. The chemical bonding analysis of the global minimum structure of B_{10} was performed by Zhai et al.[19] only for the π-system, and it was shown that this structure has 6 π-electrons and thus it is π-aromatic. We propose here an explanation of chemical bonding in B_{10} including both σ- and π-electrons. As before, let us first flatten the C_{2h} ^1A_g structure into the planar D_{2h} ^1A_g structure for simplicity and per-

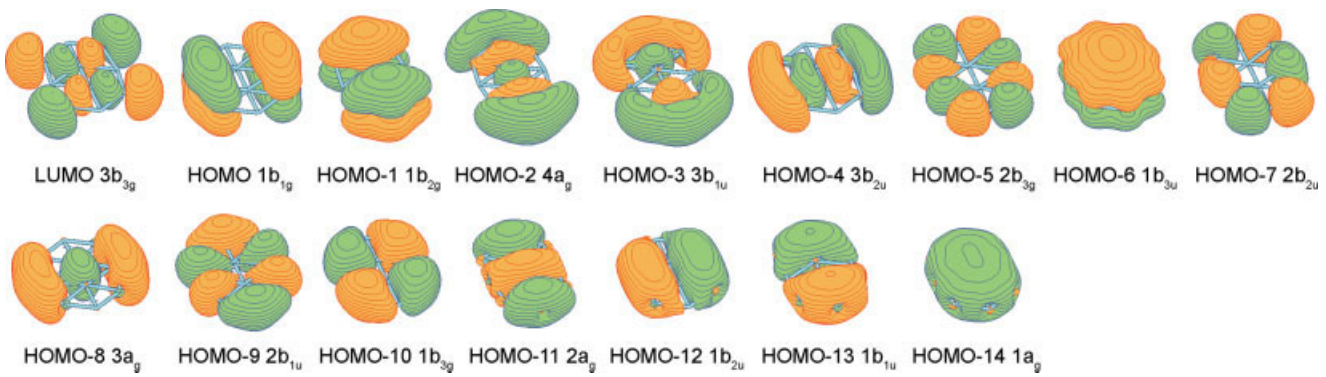

Figure 10. Molecular orbitals of the D_{2h} (^1A_g) structure of the B_{10} cluster.

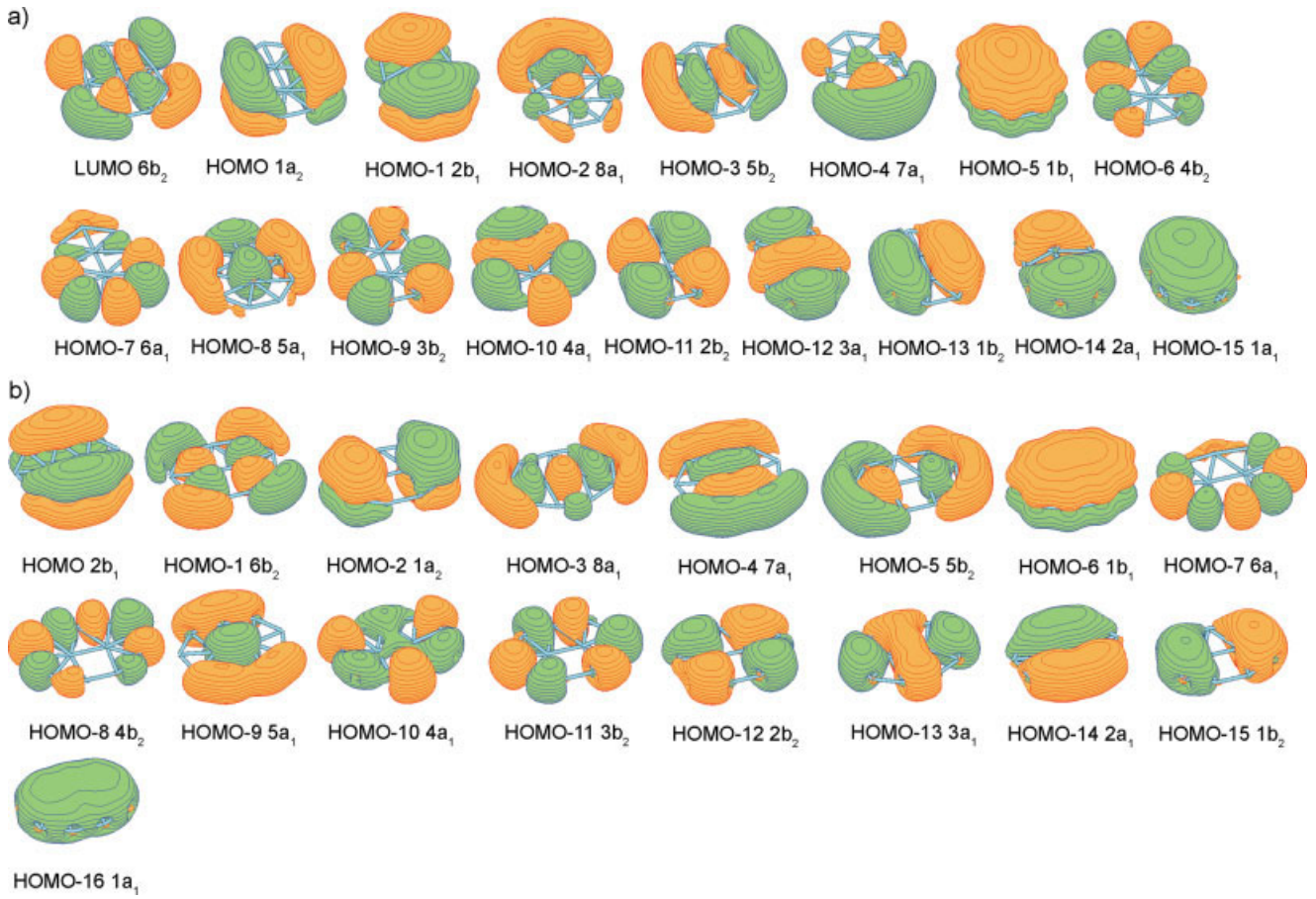

Figure 11. (a) Molecular orbitals of the C_{2v} ($^1A_1$) structure of the B_{11}^+ cation; (b) molecular orbitals of the C_{2v} ($^1A_1$) structure of the B_{11}^- anion.

form MO analysis (Fig. 10) for the planar structure. NBO analysis shows eight peripheral 2c—2e B—B bonds (ON = 1.87–1.93 |e|) and one 2c—2e B—B bond (ON = 1.52 |e|) between central atoms, which could be approximately assigned to HOMO-5 ($2b_{3g}$), HOMO-7 ($2b_{2u}$), HOMO-8 ($3a_g$), HOMO-9 ($2b_{1u}$), HOMO-10 ($1b_{3g}$), HOMO-11 ($2a_g$), HOMO-12 ($1b_{2u}$), HOMO-13 ($1b_{1u}$), and HOMO-14 ($1a_g$). Rather low occupation number for the central B—B bond shows that we should treat the existence of this bond with caution. Three MOs: HOMO ($1b_{1g}$), HOMO-1 ($1b_{2g}$), and HOMO-6 ($1b_{3u}$) are responsible for the global π-bonding and the remaining three σ-MOs: HOMO-2 ($4a_g$), HOMO-3 ($3b_{1u}$), and HOMO-4 ($3b_{2u}$) are responsible for the global σ-bonding. Thus, B_{10} is a doubly (σ- and π-) aromatic cluster with eight peripheral 2c—2e B—B bonds and one 2c—2e central B—B bond. A relatively high first singlet vertical excitation energy (1.95 eV, at TD-B3LYP/6-311 + G*) and negative NICS values (Table 1) support our description of chemical bonding in B_{10}.

We calculated the B_{10} (D_{9h}, $^1A_1'$) planar structure with only one boron atom at the center of the nine-atomic ring. The radius of the external ring was found to be 2.202 Å (B3LYP/6-311 + G*), and the central cavity is now too big to be stabilized through the accommodation of only one boron nucleus; because of that this structure is 60.5 kcal/mol higher than the global minimum structure with two boron nuclei at the center. Also, this structure is the forth order saddle point. Thus, starting from B_{10} cluster, the structures with one boron atom at the center are not low energy isomers anymore. However, the eight-membered ring is still small to favorably accommodate two boron atoms within the plane.

Ricca and Bauschlicher[42] reported a quasi-planar C_s $^1A'$ structure for the B_{11}^+ cluster (Fig. 1). In this case, the nine-atomic ring is again too small to accommodate two boron atoms within the plane. We plotted MOs of B_{11}^+ for the flattened C_{2v} $^1A_1$ ($1a_1^2 2a_1^2 1b_2^2 3a_1^2 2b_2^2 4a_1^2 3b_2^2 5a_1^2 6a_1^2 4b_2^2 1b_1^2 7a_1^2 5b_2^2 8a_1^2 2b_1^2 1a_2^2$) structure in Figure 11a. NBO analysis reveals nine 2c—2e peripheral B—B bonds (ON = 1.81–1.94 |e|) and one central B—B bond (ON = 1.53 |e|), which could be approximately assigned to 10 lowest canonical MOs (from HOMO-6 to HOMO-15). Three MOs: HOMO ($1a_2$), HOMO-1 ($2b_1$), and HOMO-5 ($1b_1$) are responsible for the global π-bonding and three MOs: HOMO-2 ($8a_1$), HOMO-3 ($5b_2$), and HOMO-4 ($7a_1$) are responsible for the global σ-bonding. Thus, the B_{11}^+ cation is a doubly aromatic system with 6σ- and 6π-delocalized electrons, nine 2c–2e B—B peripheral bonds and somewhat less pronounced central B—B bond.

The global minimum structure C_{2v} $^1A_1$ for B_{11}^- was reported by Zhai et al.[19] (Fig. 1). Our MO plots for this dianion are shown in Figure 11b. NBO analysis reveals nine 2c—2e peripheral B—B bonds (ON = 1.93–1.96 |e|) and one B—B bond between central atoms (ON = 1.56 |e|). We believe that the lowest 10 canonical MOs (from HOMO-7 to HOMO-16) are approximately responsible for the formation of these 10 B—B bonds. Three MOs: HOMO ($2b_1$), HOMO-2 ($1a_2$), and HOMO-6 ($1b_1$) are responsible for the global π-bonding, making this cluster π-aromatic as it was initially reported by Zhai et al.[19] Four MOs: HOMO-1 ($6b_2$), HOMO-3 ($8a_1$), HOMO-4 ($7a_1$), and HOMO-5 ($5b_2$) are approximately responsible for the global σ-bonding, making this system formally σ-antiaromatic. However, the shape of HOMO-1, HOMO-3, HOMO-4, and HOMO-5 hints that the globally delocalized electrons may in fact break into four localized areas (giving rise to island σ-aromaticity) over the B_{11}^- cluster, similar to σ-delocalized electrons in the B_6^{2-} cluster, where they are split into two subsystems each localized over three boron atoms. At this point, it is hard to point out which atoms in the B_{11}^- clusters belong to which regions of island σ-aromaticity.

B_{12} and B_{13}^+ Clusters

Zhai et al.[19] and Boustani[39] reported that the global minimum for B_{12} is the quasi-planar convex structure C_{3v} $^1A_1$ (Fig. 1). In this case, three central boron atoms cannot fit into the plane of the nine-membered ring. As before, let us first flatten the C_{3v} $^1A_1$ structure into the planar D_{3h} $^1A_1'$ structure for simplicity and perform MO analysis for the planar structure. NBO analysis shows nine peripheral 2c—2e B—B bonds (ON = 1.89–1.94 |e|). Unlike in B_{10}, B_{11}^+, and B_{11}^-, in B_{12} NBO analysis does not show 2c—2e B—B bonds between three central atoms. Instead, NBO analysis shows the presence of three "lone pairs" with the average occupation number about 1.1 |e| and with the total accumulation of 3.2 |e| on each of three central atoms. Such unusual accumulation of electron density could be a deficiency of the employed NBO method and a hint that two electrons on every central boron atoms could be involved into the formation of three 2c—2e B—B bonds. Let us assume that indeed, we have also three 2c—2e B—B bonds between central atoms and that makes total number of 2c—2e B—B bonds twelve. These twelve bonds take 24 out of 36 valence electrons. Molecular orbital picture (Fig. 12) also shows the presence of three globally delocalized π-MOs: HOMO-5 ($1a_2''$), HOMO-1 and HOMO-1′ ($1e''$), which reveals π-aromaticity, as it was initially reported by Zhai et al.[19] We have also six electrons on globally delocalized σ-MOs: HOMO-2 ($4a_1'$), HOMO, and HOMO′ ($5e'$), which reveals σ-aromaticity. With our previous assumptions, we can assign the B_{12} cluster as being doubly (σ- and π-) aromatic with nine 2c—2e peripheral B—B bonds and three 2c—2e central B—B bonds. We would like to stress that this description is tentative at this point. The presence of double aromaticity in B_{12} is supported by high first singlet vertical excitation energy (2.57 eV, at TD-B3LYP/6-311+G*) and highly negative NICS values (all in Table 1).

In an alternative explanation of σ-bonding in B_{12}, one may consider that central boron atoms donate their electrons to form islands of σ-aromaticity where each pair of delocalized σ-electrons is affiliated with three or four boron atoms. We need to develop new software tools for making σ-bonding analysis in such systems more precise.

The B_{13}^+ cationic cluster attracted a lot of attention, because Anderson and coworkers[25–31] reported that it has anomalously high stability and low reactivity in comparison with other cationic boron clusters. Initially, this high stability was attributed to B_{13}^+ having a filled icosahedron structure.[28] Kawai and Weare[34] have shown that a filled icosahedral of B_{13}^+ is not even a minimum on the potential energy surface using Car-Parrinello *ab initio* molecular dynamics simulations. The global minimum structure of B_{13}^+ was established by Ricca and Bauschlicher,[42] who predicted the planar C_{2v} $^1A_1$ structure (Fig. 1). Three boron atoms can fit perfectly into the plane of the 10-membered ring. Fowler and Ugalde[5a] were the first who proposed that exceptional stability and low reactivity of B_{13}^+ is related to its aromatic character. On the basis of plotted MOs, Fowler and Ugalde concluded that three doubly occupied π-MOs give six π-electrons in a round system, a situation reminiscent of benzene and the Huckel aromaticity. Aihara[6] evaluated the topological resonance energy (TRE) for π-electrons using his graph theory of aromaticity. He found that the TRE of B_{13}^+ is positive in sign and very large in magnitude: TRE = 2.959 $|\beta_{BB}|$. This number can be compared with the aromatic hydrocarbons of the similar size such as the phenalenium ($C_{13}H_9^+$) TRE = 0.410 $|\beta_{BB}|$, antracene ($C_{14}H_{10}$) TRE = 0.475 $|\beta_{BB}|$, and phenanthrene ($C_{14}H_{10}$) TRE = 0.576 $|\beta_{BB}|$. On the basis of the TRE value, B_{13}^+ is much more aromatic than polycyclic aromatic hydrocarbons of the similar size.

However, like in case of other large boron clusters, the σ-bonding has not been discussed. Molecular orbitals for the B_{13}^+ cation are plotted in Figure 13. NBO analysis shows ten 2c—2e B—B peripheral bonds (ON = 1.89–1.93 |e|) and three "lone pairs" with the average occupation number about 1.1 |e| and total accumulation of 3.2 |e| on each of three central atoms. As before, let us assume that we have also three 2c—2e B—B bonds between central atoms, which makes the total number of 2c—2e B—B bonds thirteen. These 13 bonds take 26 out of 38 valence electrons. Molecular orbital picture (Fig. 13) also shows the presence of three globally delocalized π-MOs: HOMO-6 ($1b_1$), HOMO-2 ($1a_2$), and HOMO-1 ($2b_1$), which reveals π-aromaticity, as it was previously reported by Fowler and Ugalde[5a] and Aihara.[6] We can assign six remaining electrons on HOMO-4 ($9a_1$), HOMO-3 ($6b_2$), and HOMO ($10a_1$) to globally delocalized σ-bonding. Again, we would like to stress that such chemical bonding description should be considered at this point as tentative. However, if we assume that our description is correct then the presence of double aromaticity in B_{13}^+ can explain high first singlet vertical excitation energy (2.09 eV, at TD-B3LYP/6-311 + G*), highly negative NICS values (all in Table 1), and the most importantly the anomalously high stability and low reactivity of B_{13}^+ in comparison with other cationic boron clusters observed by Anderson and coworkers.[25–31]

B_{14} and B_{15}^- Clusters

Zhai et al.[19] reported that the global minimum for B_{14} is the quasi-planar structure C_{2v} $^1A_1$ (Fig. 1). We performed MO anal-

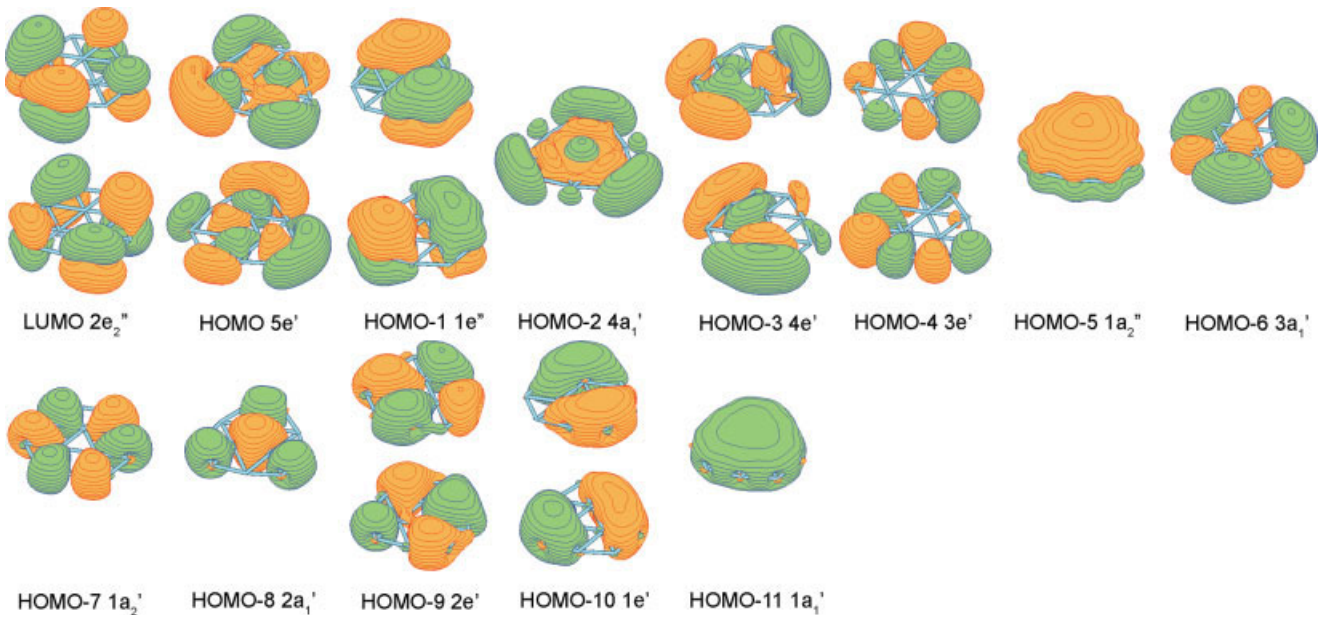

Figure 12. Molecular orbitals of the D_{3h} ($^1A_1'$) structure of the B_{12} cluster.

ysis for the planar D_{2h} (^1A_g) structure (Fig. 14). NBO analysis shows 10 peripheral 2c—2e B—B bonds (ON = 1.88–1.95 |e|). It also shows the presence of three "lone pairs" with the average occupation number about 1.1 |e| and the total accumulation of 2.9–3.3 |e| on each of four central atoms. Like before, let us assume that there are four 2c—2e B—B bonds between central atoms. That makes total number of 2c—2e B—B bonds 14. These 14 bonds take 28 out of 42 valence electrons. Molecular orbital picture (Fig. 14) also shows the presence of four globally delocalized π-MOs: HOMO-10 ($1b_{3u}$), HOMO-4 ($1b_{1g}$), HOMO-3 ($1b_{2g}$), and HOMO ($2b_{3u}$), which reveals global π-antiaromaticity, as it was previously reported by Zhai et al.[19] The global π-antiaromaticity results in the formation of small areas of π-aromaticity (island aromaticity). The remaining six electrons occupy globally delocalized σ-MOs: HOMO-6 ($5a_g$), HOMO-2 ($5b_{2u}$), and HOMO-1 ($6a_g$), which reveals σ-aromaticity. Thus,

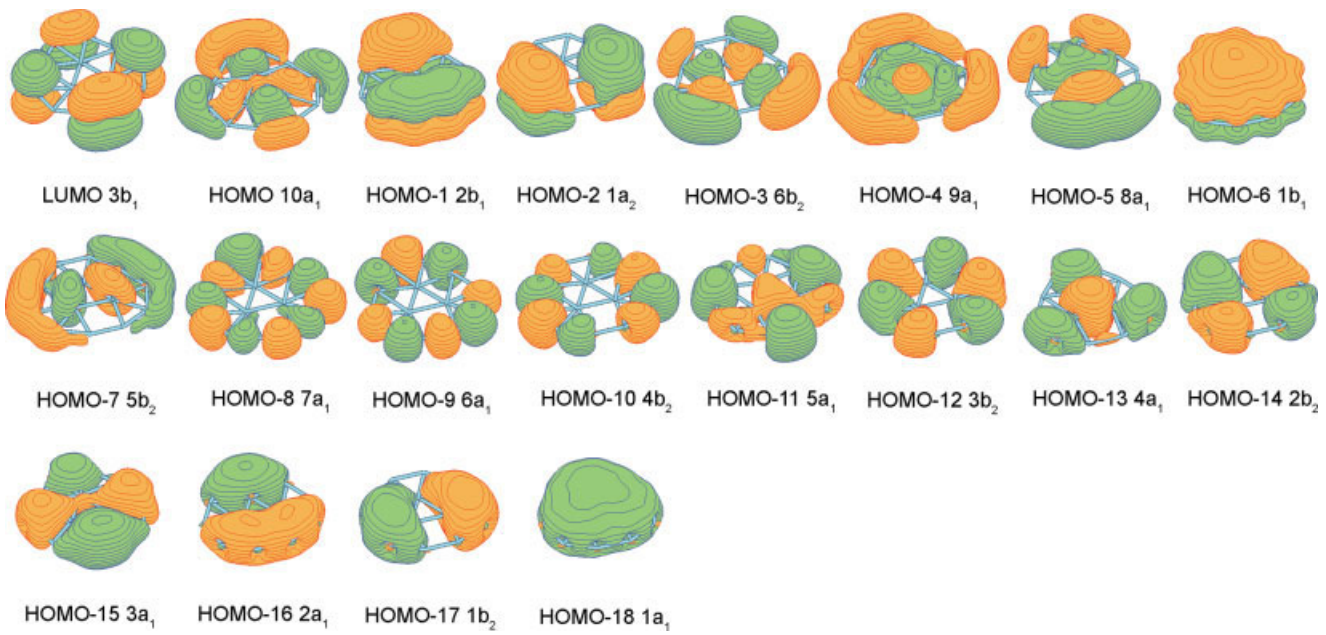

Figure 13. Molecular orbitals of the C_{2v} ($^1A_1$) structure of the B_{13}^+ cation.

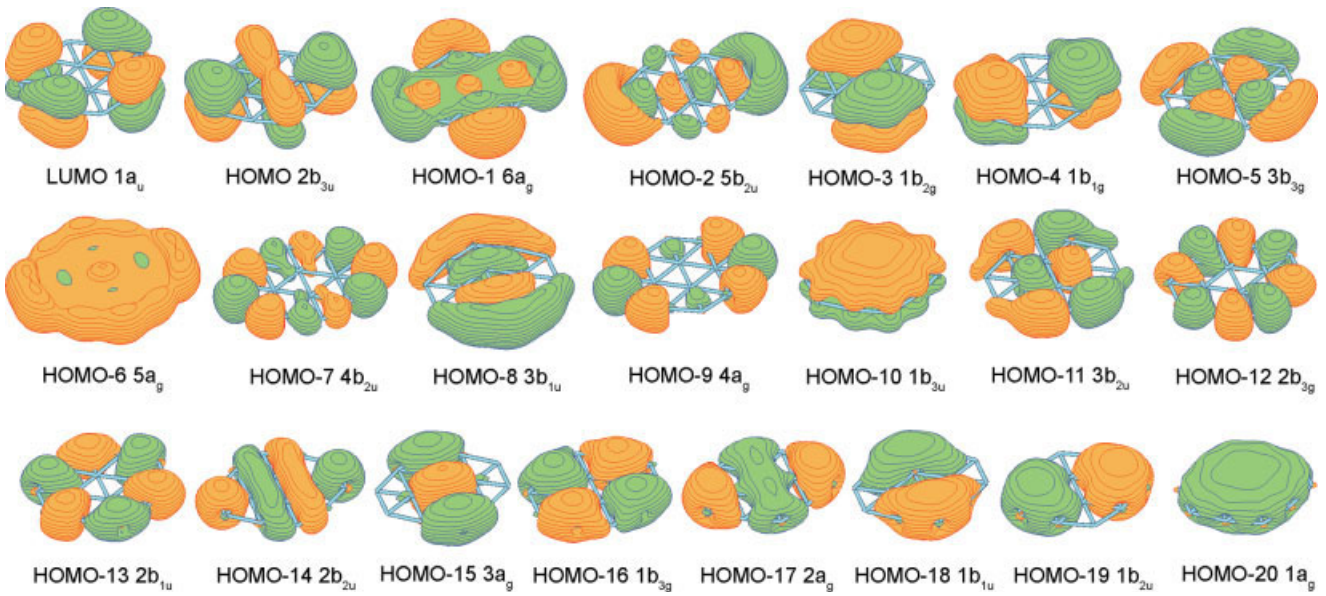

Figure 14. Molecular orbitals of the D_{2h} (^1A_g) structure of the B_{14} cluster.

we can tentatively assign the B_{14} cluster as having conflicting ((σ-aromatic and π-antiaromatic) aromaticity with 10 2c—2e peripheral B—B bonds and four 2c—2e central B—B bonds.

Zhai et al.[19] reported that the global minimum for B_{15}^- is the quasi-planar structure C_1 ^1A (Fig. 1). We performed MO analysis for the planar C_{2v} ($^1A_1$) structure (Fig. 15). NBO analysis shows 11 peripheral 2c—2e B—B bonds (ON = 1.88–1.95 |e|). It also shows the presence of the three "lone pairs" with the average occupation number about 1.1 |e| with the total accumulation of 2.9–3.3 |e| on each of four central atoms. Let us assume that we have also four 2c—2e B—B bonds between central atoms. That makes total number of 2c—2e B—B bonds 15. These 15 bonds take 30 out of 46 valence electrons. Molecular orbital picture (Fig. 15) shows the presence of four globally delocalized π-MOs: HOMO-11 ($1b_1$), HOMO-5 ($1a_2$), HOMO-2 ($2b_1$), and HOMO-1 ($3b_1$), which reveals global π-antiaromaticity. We have also eight

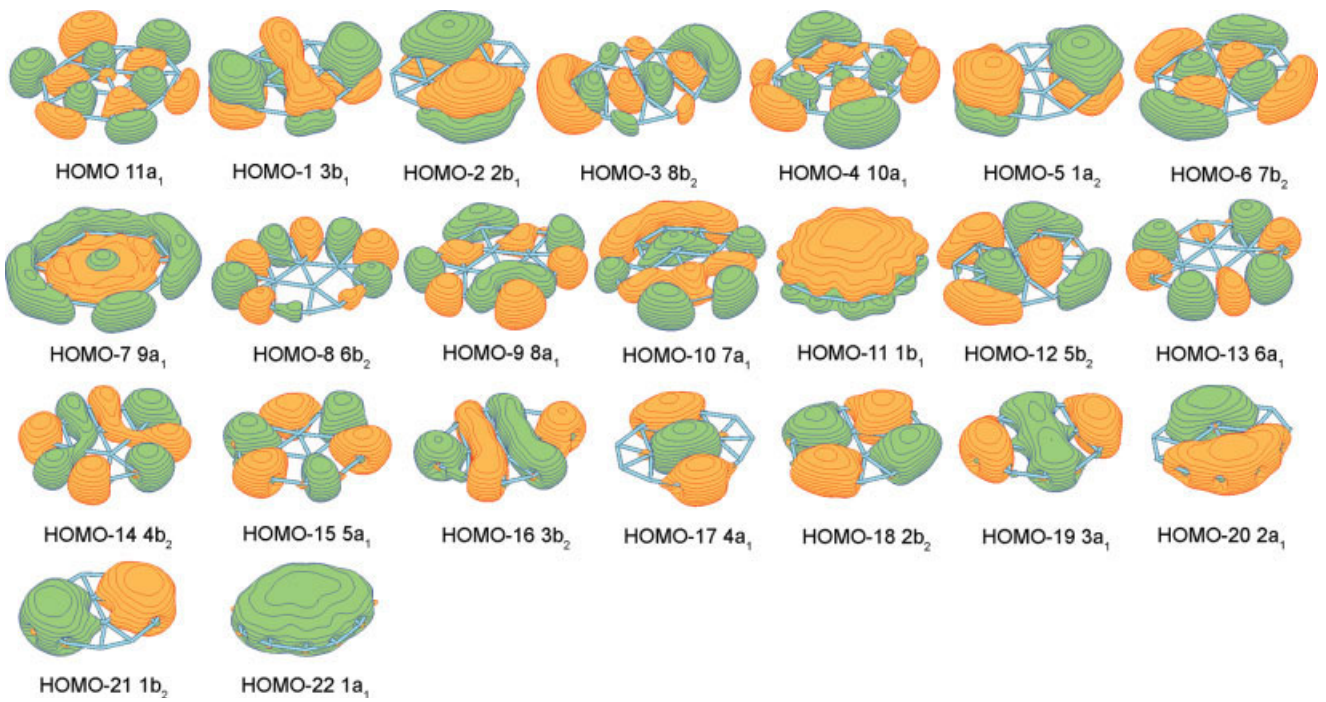

Figure 15. Molecular orbitals of the C_{2v} ($^1A_1$) structure of the B_{15}^- anion.

electrons on globally delocalized σ-MOs: HOMO ($11a_1$), HOMO-3 ($8b_2$), HOMO-4 ($10a_1$), and HOMO-7 ($9a_1$), which reveals global σ-antiaromaticity. Thus, we can tentatively consider the B_{15}^- cluster as being doubly (σ- and π-) antiaromatic with eleven 2c—2e peripheral B—B bonds and four 2c—2e central B—B bonds. Again the π- and σ-antiaromaticity result in the formation of small areas of aromaticity (island aromaticity).

Overview

On the basis of chemical bonding analysis performed for B_3^+, B_3^-, B_4, B_4^{2-}, B_5^+, B_5^-, B_6^{2+}, B_6, B_6^{2-}, B_7^+, B_7^-, B_8, B_8^{2-}, B_9^-, B_{10}, B_{11}^+, B_{11}^-, B_{12}, B_{13}^+, B_{14}, and B_{15}^- clusters in this work, we propose the next chemical bonding model for planar or quasi-planar boron clusters:

- The number of 2c—2e peripheral B—B bonds in all considered here planar or quasi-planar clusters is equal to the number of peripheral edges.
- There are globally delocalized π-MOs, which make a cluster either globally π-aromatic if it has $4n + 2$ π-electrons or globally antiaromatic if it has $4n$ π-electrons for singlet coupled electrons. For triplet coupled π-electrons, the number of electrons should satisfy the inverse $4n$ rule for aromaticity.
- There are globally delocalized σ-MOs, which make a cluster either globally σ-aromatic if it has $4n + 2$ σ-electrons or globally antiaromatic if it has $4n$ σ-electrons for singlet coupled electrons. For triplet coupled σ-electrons, the number of electrons should satisfy the inverse $4n$ rule for aromatic systems.

This bonding model works well for B_3^+–B_9^- clusters. Some boron clusters can be doubly (σ- and π-) aromatic: B_3^-, B_4, B_5^+, B_7^+, B_7^-, B_8, B_8^{2-}, and B_9^-. Some clusters can be globally doubly antiaromatic, for example, B_6^{2-}. Global antiaromaticity can be also described in terms of formation of areas of island aromaticity. In the B_6^{2-} clusters, the globally delocalized π-and σ- electrons can be localized over two areas composed of three boron atoms. Some clusters may have conflicting aromaticity, such as B_5^- (which is π-aromatic and σ-antiaromatic). For larger clusters, in addition to peripheral 2c—2e B—B bonds globally delocalized π-MOs, and globally delocalized σ-MOs, we can introduce one 2c—2e central B—B bond (B_{10}, B_{11}^+, B_{11}^-), three 2c—2e central B—B bonds (B_{12}, B_{13}^+) or four 2c—2e central B—B bonds (B_{14}, B_{15}^-). The presence of central 2c—2e bonds was confirmed up to certain degree only in B_{10}, B_{11}^+, and B_{11}^- clusters. In other large clusters it was postulated. There is an alternative approach in which electrons located at central boron atoms are thought to participate in global delocalization resulting in formation of several areas with island σ-aromaticity.

We would also like to point out that there is no conflict between our assignment of planar boron clusters with $4n$ π-electrons to antiaromatic and Aihara et al. assignment of the same molecules to aromatic. The disagreement is purely semantic. We are talking about global antiaromaticity of boron clusters with $4n$ π-electrons. We, however, agree that a globally π-antiaromatic molecule such as B_6^{2-} could have islands of π-aromaticity. The island π-aromaticity is responsible for the high TRE = 0.549 $|\beta_{BB}|$ energy in B_6^{2-}. However, to explain low symmetry (D_{2h} instead of D_{6h}) of B_6^{2-}, we must consider this cluster as being globally π-antiaromatic. The same is true for larger π-antiaromatic clusters. Similarly, in B_5^-, the high TRE = 1.058 $|\beta_{BB}|$ cannot explain the low symmetry (C_{2v} instead of D_{5h}) of B_5^- as well as the small first singlet vertical excitation energy. The σ-electrons must be included in chemical bonding analysis. When the global σ-antiaromaticity in the B_5^- cluster is recognized, the low symmetry C_{2v} structure and small first singlet vertical excitation energy have rather simple explanation, which is not possible if only π-aromaticity in this cluster is considered.

Appropriate geometric fit is also an essential factor, which determines the shape of the most stable structures. In all the boron clusters considered here, the peripheral atoms form planar cycles. Peripheral 2c—2e B—B bonds are built up from s–p hybrid atomic orbitals and this enforces the planarity of the cycle. If the given number of central atoms (1, 2, 3, or 4) can perfectly fit the central cavity then the overall structure is planar. Otherwise, central atoms come out of the plane of the cycle.

Initially, from B_3 to B_6 the cyclic (perfect or distorted depending on their aromatic or antiaromatic character) structures correspond to global minima. In the B_6 cluster, in addition to cyclic structures, we observe the emergence of a new type of structure, pentagonal pyramid, which now corresponds to the global minimum. The planar pentagon structure with the boron atom located at the center of the pentagon is not a minimum because the cavity inside of the pentagon is too small to favorably accommodate a boron atom at the center. The cyclic B_7^+ D_{7h} ($^3A_2'$) structure is significantly higher (63.4 kcal/mol at B3LYP/6-311 + G*) in energy than the global minimum C_{6v} ($^1A_1'$) structure, because of unsupported dangling electron density at the center of the cycle. Thus, the cyclic structures are not favorable anymore beyond six boron atoms. Starting with B_8, the central cavity can favorably accommodate one boron atom at the center of the appropriate polygon leading to planar highly symmetric global minimum structures. Starting from B_{10} cluster, the structures with one boron atom at the center are not low energy isomers anymore, because it takes more than one boron nucleus to make a good fit for the central cavity.

We believe that this approach in which we combine 2c—2e bonds (or lone pairs) with global (or island) π- and σ-aromaticity is a perspective way to characterize chemical bonding in large boron clusters and could potentially become a useful tool in addition to π-delocalization and π-aromaticity in case of other new planar clusters such as hyparenes,[2b,2c] aromatic boron wheels with more than one carbon atom at the center,[80,81] and fen-shaped B_nE_2Si (E = CH, BH, or Si, n = 2–5) clusters.[82]

Acknowledgments

Computer time from the Center for High Performance Computing at Utah State University is gratefully acknowledged. DYZ wishes to thank Utah State University for a Presidential Fellowship.

References

1. (a) Boldyrev, A. I.; Wang, L. S. Chem Rev 2005, 106, 3716; (b) Li, X.; Kuznetsov, A. E.; Zhang, H. F.; Boldyrev, A. I.; Wang, L. S. Science 2001, 291, 859; (c) Kuznetsov, A. E.; Birch, K. A.; Boldyrev, A. I.; Li, X.; Zhai, H.-J.; Wang, L. S. Science 2003, 300, 622; (d) Boldyrev, A. I.; Kuznetsov, A. E. Inorg Chem 2002, 41, 532; (e) Alexandrova, A. N.; Boldyrev, A. I. J Phys Chem A 2003, 107, 554.
2. (a) Chen, Z.; Wannere, C. S.; Corminboeuf, C.; Puchta, R.; Schleyer, P. v. R. Chem Rev 2005, 106, 3842; (b) Exner, K.; Schleyer, P. v. R. Science 2000, 1937, 290; (c) Wang, Z.-X.; Schleyer, P. v. R. Science 2001, 292, 2465; (d) Tanaka, H.; Neukermans, S.; Janssens, E.; Silverans, R. E.; Lievens, P. J Am Chem Soc 2003, 125, 2863.
3. (a) Tsipis, C. A. Coord Chem Rev 2005, 249, 2740; (b) Tsipis, A. C.; Tsipis, C. A. J Am Chem Soc 2003, 125, 1136.
4. (a) Jemmis, E. D.; Jayasree, E. G. Acc Chem Res 2003, 36, 816; (b) Balakrishnarajan, M. M.; Hoffmann, R.; Pancharatna, P. D.; Jemmis, E. D. Inorg Chem 2003, 42, 4650; (c) Jemmis, E. D.; Balakrishnarajan, M. M.; Pancharatna, P. D. Chem Rev 2002, 102, 93.
5. (a) Fowler, J. E.; Ugalde, J. M. J Phys Chem A 2000, 104, 397; (b) Mercero, J. M.; Ugalde, J. M. J Am Chem Soc 2004, 126, 3380.
6. Aihara, J. J Phys Chem A 2001, 105, 5486.
7. (a) Fowler, P. W.; Havenith, R. W. A.; Steiner, E. Chem Phys Lett 2001, 342, 85; (b) Havenith, R. W. A.; Fowler, P. W.; Steiner, E. Chem—Eur J 2002, 8, 1068; (c) Fowler, P. W.; Havenith, R. W. A.; Steiner, E. Chem Phys Lett 2002, 359, 530; (d) Havenith, R. W. A.; van Lenthe, J. H. Chem Phys Lett 2004, 385, 198; (e) Havenith, R. W. A.; De Proft, F.; Fowler, P. W.; Geerling, P. Chem Phys Lett 2005, 407, 391.
8. (a) Juselius, J.; Straka, M.; Sundholm, D.; J Phys Chem A 2001, 105, 9939; (b) Lin, Y.-C.; Juselius, J.; Sundholm, D.; J Chem Phys 2005, 122, 214308; (c) Lin, Y.-C.; Sundholm, D.; Juselius, J.; Cui, L.-F.; Li, X.; Zhai, H.-J.; Wang, L. S. J Phys Chem A 2006, 110, 4244.
9. Zhan, C.-G.; Zheng, F.; Dixon, D. A. J Am Chem Soc 2002, 124, 147.
10. Santos, J. C.; Andres, J.; Aizman, A.; Fuentealba, P. J Chem Theory Comput 2005, 1, 83.
11. (a) Datta, A.; Pati, S. K.; J Phys Chem A 2004, 108, 9527; (b) Datta, A.; Pati, S. K. J Am Chem Soc 2005, 127, 3496; (c) Datta, A.; Pati, S. K.; J Chem Theory Comput 2005, 1, 824; (d) Datta, A.; John, N. S.; Kulkarni, G. U.; Pati, S. K. J Phys Chem A 2005, 109, 11647; (e) Rehaman, A.; Datta, A.; Mallajosyulu, S. S.; Pati, S. K. J Comput Theory Comput 2006, 2, 30.
12. (a) Havenith, R. W. A.; Fowler, P. W.; Steiner, E.; Shetty, S.; Kanhere, D.; Pal, S. Phys Chem Chem Phys 2004, 6, 285; (b) Shetty, S.; Kar, R.; Kanhere, D. G.; Pal, S. J Phys Chem A 2006, 110, 252.
13. (a) Hu, X. B.; Li, H. R.; Liang, W. C.; Han, S. J.; Chem Phys Lett 2004, 397, 180; (b) Hu, X.; Li, H.; Liang, W.; Han, S. Chem Phys Lett 2005, 402, 539; (c) Hu, X. B.; Li, H. R.; Liang, W. C.; Han. S. J. New J Chem 2005, 29, 1295; (d) Wang, F.-F.; Li, Z.-R.; Wu, D.; Sun, X.-Y.; Chen, W.; Li, Y.; Sun, C.-C. Chem Phys Chem 2006, 7, 1136.
14. (a) Zhai, H. J.; Wang, L. S.; Alexandrova, A. N.; Boldyrev, A. I.; Zakrzewski, V. G. J Phys Chem A 2003, 107, 9319; (b) Kuznetsov, A. E.; Boldyrev, A. I. Struct Chem 2002, 13, 141.
15. Zhai, H. J.; Wang, L. S.; Alexandrova, A. N.; Boldyrev, A. I. J Chem Phys 2002, 117, 7917.
16. Alexandrova, A. N.; Boldyrev. A. I.; Zhai, H. J.; Wang, L. S.; Steiner, E.; Fowler, P. W. J Phys Chem A 2003, 107, 1359.
17. Alexandrova, A. N.; Boldyrev, A. I.; Zhai, H. J.; Wang, L. S. J Phys Chem A 2004, 108, 3509.
18. Zhai, H. J.; Wang. L. S.; Alexandrova, A. N.; Boldyrev, A. I. Angew Chem Int Ed 2003, 42, 6004.
19. Zhai, H. J.; Kiran, B.; Li, J.; Wang, L. S. Nat Mater 2003, 2, 827.
20. Aihara, J.; Kanno, H.; Ishida, T. J Am Chem Soc 2005, 127, 13324.
21. Alexandrova, A. N.; Zhai, H.-J.; Wang, L. S.; Boldyrev, A. I. Inorg Chem 2004, 43, 3588.
22. Alexandrova, A. N.; Boldyrev, A. I.; Zhai, H.-J.; Wang, L. S. J Chem Phys 2005, 122, 054313.
23. Alexandrova, A. N.; Koyle, E.; Boldyrev, A. I. J Mol Mod 2006, 12, 569.
24. Zhai, H.-J.; Wang, L. S.; Zubarev, D. Yu.; Boldyrev, A. I. J Phys Chem A 2006, 110, 1689.
25. Hanley, L.; Anderson, S. L. J Phys Chem 1987, 91, 5161.
26. Hanley, L.; Anderson, S. L. J Chem Phys 1988, 89, 2848.
27. Hanley, L.; Whitten, J. L.; Anderson, S. L. J Phys Chem 1988, 92, 5803.
28. Hintz, P. A.; Ruatta, S. A.; Anderson, S. L. J Chem Phys 1990, 92, 292.
29. Ruatta, S. A.; Hintz, P. A.; Anderson, S. L. J Chem Phys 1991, 94, 2833.
30. Hintz, P. A.; Sowa, M. B.; Ruatta, S. A.; Anderson, S. L. J Chem Phys 1991, 94, 6446.
31. Sowa-Resat, M. B.; Smolanoff, J.; Lapiki, A.; Anderson, S. L. J Chem Phys 1997, 106, 9511.
32. Kawai, R.; Weare, J. H. J Chem Phys 1991, 95, 1151.
33. La Placa, S. J.; Roland, P. A.; Wynne, J. J Chem Phys Lett 1992, 190, 163.
34. Kawai, R.; Weare, J. H. Chem Phys Lett 1992, 191, 311.
35. Martin, J. M. L.; François, J. P.; Gijbels, R. Chem Phys Lett 1992, 189, 52.
36. Kato, H.; Yamashita, K.; Morokuma, K. Chem Phys Lett 1992, 190, 361.
37. Roland, P. A.; Wynne, J. J. J Chem Phys 1993, 99, 8599.
38. Kato, H.; Yamashita, K.; Morokuma, K. Bull Chem Soc Jpn 1993, 66, 3358.
39. Boustani, I. Int J Quantum Chem 1994, 52, 1081.
40. Boustani, I. Chem Phys Lett 1995, 233, 273.
41. Boustani, I. Chem Phys Lett 1995, 240, 135.
42. Ricca, A.; Bauschlicher, C. W., Jr. Chem Phys 1996, 208, 233.
43. Boustani, I. Surf Sci 1997, 370, 355.
44. Boustani, I. Phys Rev B 1997, 53, 16426.
45. Nie, J.; Rao, B. K.; Jena, P. J Chem Phys 1997, 107, 132.
46. Gu, F. L.; Yang, X.; Tang, A.-C.; Jiao, H.; Schleyer, P. V. R. J Comput Chem 1998, 19, 203.
47. Reis, H.; Papadopoulos, M. G.; Boustani, I. Int J Quant Chem 2000, 78, 131.
48. Yang, C. L.; Zhu, Z. H. J Mol Struct (Theochem) 2001, 571, 225.
49. Cao, P.-L.; Zhao, W.; Li, B.; Song, X.-B.; Zhou, X.-Y. J Phys: Condens Matter 2001, 13, 5065.
50. Li, Q. S.; Jin, H. W. J Phys Chem A 2002, 106, 7042.
51. Ma, J.; Li, Z.; Fan, K.; Zhou, M. Chem Phys Lett 2003, 372, 708.
52. Jin, H. W.; Li, Q. S.; Phys Chem Chem Phys 2003, 5, 1110.
53. Li, Q. S.; Jin, Q. J Phys Chem A 2004, 108, 855.
54. Li, Q. S.; Jin, Q.; Luo, Q.; Tang, A. C.; Yu, J. K.; Zhang, H. X. Int J Quant Chem 2003, 94, 269.
55. Wyss, M.; Riaplov, E.; Batalov, A.; Maier, J. P.; Weber, T.; Meyer, W.; Rosmus, P. J Chem Phys 2003, 119, 9703.
56. Cias, P.; Araki, M.; Denisov, A.; Maier, J. P. J Chem Phys 2004, 121, 6776.
57. Batalov, A.; Fulara, J.; Shnitko, I.; Maier, J. P. Chem Phys Lett 2005, 404, 315.
58. Gillery, C.; Linguerri, R.; Rosmus, P.; Maier, J. P. Z. Phys Chem 2005, 219, 467.

59. Li, Q.-S.; Gong, L.-F. J Phys Chem A 2004, 108, 4322.
60. Li, Q.-S.; Gong, L.-F.; Gao, Z.-M. Chem Phys Lett 2004, 390, 220.
61. Li, Q.; Zhao, Y.; Xu, W.; Li, N. Int J Quant Chem 2005, 101, 219.
62. Lau, K. C.; Deshpande, M.; Pandey, R. Int J Quant Chem 2005, 102, 656.
63. Alexandrova, A. N.; Boldyrev, A. I.; Zhai, H.-J.; Wang, L. S. Coord Chem Rev 2006, 250, 2811.
64. Reed, A. E.; Curtiss, L. A.; Weinhold, F. Chem Rev 1988, 88, 899.
65. Parr, R. G.; Yang, W. Density-Functional Theory of Atoms and Molecules; Oxford University Press: Oxford, 1989.
66. Becke, A. D. J Chem Phys 1993, 98, 5648.
67. Perdew, J. P.; Chevary, J. A.; Vosko, S. H.; Jackson, K. A.; Pederson, M. R.; Singh, D. J.; Fiolhais, C. Phys Rev B 1992, 46, 6671.
68. Clark, T.; Chandrasekhar, J.; Spitznagel, G.W.; Schleyer, P. v. R. J Comput Chem 1983, 4, 294.
69. Frisch, M. J.; Pople, J. A.; Binkley, J. S. J Chem Phys 1984, 80, 3265.
70. Schleyer, P. v. R.; Maerker, C.; Dransfeld, A.; Jiao, H.; Hommes, N. J. R. v. E. J Am Chem Soc 1996, 118, 6317.
71. Bauernshmitt, R.; Alrichs, R. Chem Phys Lett 1996, 256, 454.
72. Casida, M. E.; Jamorski, C.; Casida, K. C.; Salahub, D. R. J Chem Phys 1998, 108, 4439.
73. Frisch, M. J.; Trucks, G. M.; Schlegel, H. B.; Scuseria, G. E.; Robb, M. A.; Cheeseman, J. R.; Montgomery, J. A., Jr.; Vreven, T.; Kudin, K. N.; Burant, J. C.; Millam, J. M.; Iyengar, S. S.; Tomasi, J.; Barone, V.; Mennucci, B.; Cossi, M.; Scalmani, G.; Rega, N.; Petersson, G. A.; Nakatsuji, H.; Hada, M.; Ehara, M.; Toyota, K.; Fakuda, R.; Hasegawa, J.; Ishida, M.; Nakajima, T.; Honda, Y.; Kitao, O.; Nakai, H.; Klene, M.; Li, X.; Knox, J. E.; Hratchian, H. P.; Cross, J. B.; Adamo, C.; Jaramillo, J.; Gomperts, R.; Stratmann, R. E.; Yazyev, O.; Austin, A. J.; Cammi, R.; Pomelli, C.; Ochterski, J. W.; Ayala, P. Y.; Morokuma, K.; Voth, G. A.; Salvador, P.; Dannenberg, J. J.; Zakrzewski, V. G.; Dapprich, S.; Daniels, A. D.; Strain, M. C.; Farkas, O.; Malick, D. K.; Rabuck, A. D.; Raghavachari, K.; Foresman, J. B.; Ortiz, J. V.; Cui, Q.; Baboul, A. G.; Clifford, S.; Cioslowski, J.; Stefanov, B. B.; Liu, G.; Liashenko, A.; Piskorz, P.; Komaromi, I.; Martin, R. L.; Fox, D. J.; Keith, T.; Al-Laham, M. A.; Peng, C. Y.; Nanayakkara, A.; Challacombe, M.; Gill, P. M. W.; Johnson, B. G.; Chen, W.; Wong, M. W.; Gonzales, C.; Pople, J. A. Gaussian 03 (revision A. 1); Gaussian, Inc.: Pittsburgh, PA, 2003.
74. Schaftenaar, G. MOLDEN3.4; CAOS/CAMM Center: The Netherlands, 1998.
75. (a) Chandrasekhar, J.; Jemmis, E. D.; Schleyer, P. V. R. Tetrahedron Lett 1979, 39, 3707; (b) Schleyer, P. v. R.; Jiao, H.; Glukhovtsev, M. N.; Chandrasekhar, J.; Kraka, E. J Am Chem Soc 1994, 116, 10129.
76. Martin-Santamaria, S.; Rzepa, H. S. Chem Commun 2000, 1503.
77. Präsang, C.; Hofmann, M.; Geiseler, G.; Massa, W.; Berndt, A. Angew Chem Int Ed 2002, 41, 1526; (b) Präsang, C.; Mlodzianowska, A.; Sahin, Y.; Hofmann, M.; Geiseler, G.; Massa, W.; Berndt, A. Angew Chem Int Ed 2002, 41, 3380; (c) Mesbah, W.; Präsang, C.; Hofmann, M.; Geiseler, G.; Massa, W.; Berndt, A. Angew Chem Int Ed 2003, 42, 1717; (e) Hofmann, M.; Berndt, A. Heteroatom Chem 2006, 17, 224.
78. Minkin, V. I.; Minyaev, R. M. Mendeleev Comm 2004, 14, 43.
79. Minyaev, R. M.; Gribanova, T. N.; Starikov, A. G.; Minkin, V. I. Mendeleev Comm 2001, 11, 213.
80. Erhardt, S.; Frenking, G.; Chen, Z.; Schleyer, P. v. R. Angew Chem Int Ed 2005, 44, 1078.
81. Wu, Y.-B.; Yuan, C.-X.; Yang, P. J Mol Struct (Theochem) (in press).
82. Li, S.-D.; Miao, C.-C.; Guo, J.-C.; Ren, G.-M. J Am Chem Soc 2004, 126, 16227.